THE OXIDATION KINETICS OF FREE

FALLING IRON DROPLETS

THE OXIDATION KINETICS OF FREE

FALLING IRON DROPLETS

by

SATINDER KUMAR VIG, B.Tech.

A Thesis

Submitted to the Faculty of Graduate Studies

in Partial Fulfilment of the Requirements

for the Degree

Master of Engineering

McMaster University

September 1969

MASTER OF ENGINEERING (1969) McMASTER UNIVERSITY
(Metallurgical Engineering) Hamilton, Ontario.

TITLE: The Oxidation Kinetics of Free Falling Iron Droplets

AUTHOR: Satinder Kumar Vig, B.Tech.

SUPERVISOR: Dr. W-K. Lu

NUMBER OF PAGES: x, 67

SCOPE AND CONTENTS:

Levitation melting was used to study the oxidation kinetics of
free falling iron droplets. Single droplets of Armco iron were
deoxidized and allowed to fall through oxidizing columns of known
heights and then quenched in Silicone Oil. The rate of oxygen pick
up by a droplet was found to be dependent upon its initial temperature,
its size, and the composition of the reacting gas. The proposed
mechanism is presented with kinetic data.

TABLE OF CONTENTS

LIST OF ILLUSTRATIONS·

LIST OF TABLES

NOMENCLATURE

A	:	Surface area of the droplet	cm^2.
C_D	:	Dimensionless drag coefficient	
C_p	:	Heat capacity at constant pressure	Cal./gm.mole -°K.
d	:	Droplet diameter	cm.
D_{AB}	:	Diffusion coefficient of species A	cm^2./sec.
g	:	Gravitational constant	cm./sec^2.
h	:	Convective heat transfer coefficient	Cal.$sec.^{-1} cm.^{-2} \, °K^{-1}$
H	:	Height of fall or distance travelled	cm.
k	:	Thermal conductivity of gas	Cal.$sec.^{-1} cm.^{-1} \, °K^{-1}$
M_d	:	Mass of the droplet	gm.
M_g	:	Mass of the gas displaced	gm.
Nu	:	Nusselt number $= \dfrac{h.d}{k}$	
P	:	Pressure	atm.
Pr	:	Prandtl number $= \dfrac{C_p \cdot \mu_g}{k}$	
R	:	Gas constant	cm^3.-atm./gm.mole/°K
Re	:	Reynolds number $= \dfrac{\rho.v.d}{\mu_g}$	
T_d	:	Droplet temperature	°K
T_E	:	Effective temperature	°K
T_f	:	Film temperature	°K
T_H	:	Droplet temperature at the separating diaphragm	°K
t	:	Time	Sec.
v	:	Velocity	cm./sec.

X_A	:	Mole fraction of species A	
ρ_g	:	Density of the gas	$gm./cm.^3$
ρ_d	:	Density of the droplet	$gm./cm.^3$
μ_g	:	Viscosity of the gas	Poise
σ	:	Stefans - Boltzman Constant	$Cal.sec.^{-1} cm.^{-2} \, °K^{-4}$
ϵ	:	Emissivity of the droplet	

CHAPTER I

INTRODUCTION

Steelmaking is essentially an oxidation process for the removal of Si, Mn, C, S and P from blast furnace metal and scrap to give steel of a desired composition. Broadly the steelmaking processes may be divided into the following:

1. <u>Hearth Processes</u>: Open-hearth, electric arc and Kaldo processes fall into this category. These processes are mainly controlled by the reaction at the slag-metal interface. In general, the hearth type processes are relatively slow since the oxygen required for refining must diffuse through the slag phase and slag-metal interface into the melt before refining reaction can occur.

2. <u>Convertor Processes</u>: The acid Bessemer convertor with a dry inactive silicon saturated slag is controlled by the reaction at the gas-metal interface.

The most important steelmaking processes today, involve both slag-metal and gas-metal reactions e.g. the L.D. (or B.O.F.), the open hearth and electric arc furnaces with oxygen injection and the basic Bessemer convertor with a fluid active slag. In these processes, slag metal reactions are important for good phosphorus removal while gas-metal reactions accelerate the overall refining process. In general the convertor type processes are relatively fast, since oxygen is fed directly into the metal phase.

3. <u>Continuous Processes</u>: In the Tower process[1] the refining is done by a spray technique in which the impure metal is dispersed as

1

droplets and oxidation allowed to occur as droplets fall under gravity through air or oxygen.

In the WORCRA[2] continuous steelmaking process steel is made continuously by sequentially lancing with oxygen a slowly flowing stream of hot metal over which the slag flows counter-currently.

The IRSID[3] continuous refining process is based on a large increase of the interfacial area of the suspended metal droplets in a mass of slag. For this purpose a continuous slag-metal-gas complex is created.

The BISRA[4-7] spray steelmaking process involves the atomization of a stream of hot metal by high velocity jets of oxygen. The droplets formed fall and accelerate in an oxidizing atmosphere, pass through an oxidizing slag and coalesce in a molten pool. In this way a large surface area of metal is exposed to an oxygen environment and the refining reactions for removal of Si, Mn, C and P take only seconds to complete rather than minutes as in the convertor processes or hours as in the hearth processes.

In the study of inclusions, people have found that some inclusions are more likely to be the product of reoxidation during teeming and pouring rather than the product of deoxidation. Products of reoxidation formed during the casting operations are likely to be much more troublesome than the deoxidation products, since there is a greater tendency for the former to remain entrapped within the solidifying metal, whereas the latter have more opportunity to separate out into the slag phase while the steel is still in the ladle.

In steelmaking operations it is desirable to prevent the oxidation

of metal streams during the pouring and teeming stages because it will change the composition of the alloys and probably result in dirtier ingots. On the contrary, in the new "Spray Steelmaking" process of BISRA rapid oxidation of impurities present in blast furnace iron is to be preferred. In both the aforementioned cases, liquid metal falls from one container to the other. Therefore the time available for reaction is very small, in the order of a fraction of a second, and the reaction rates are extremely high.

In order to control the mode and extent of such reactions, it is essential to know the kinetics, in addition to the thermodynamics, of oxidation of liquid iron alloys. However, the oxidation kinetics of impurities, except in extremely high concentrations, in iron alloys would be difficult to understand without information concerning the behaviour of the solvent, iron, under similar experimental conditions.

In this study a levitation apparatus has been designed to investigate the fundamental nature of the oxidation kinetics of free falling iron droplets.

CHAPTER II

LITERATURE REVIEW

Several attempts have been made to refine blast furnace iron rapidly by increasing the surface area available for reactions. This has been done by splitting the metal streams into droplets which fall through an oxidizing atmosphere[1, 3-7].

In the "spray steelmaking" process of BISRA, the metal stream is broken up by high-velocity jets of oxygen, and the spray of small droplets produced is refined a) in the turbulent spray zone, b) during free fall in an oxidizing atmosphere, c) on passage through a molten slag and d) in a receiving ladle.

In order to control such a process it is essential to know the mode and extent of reactions during these stages. To this end, attempts have been made by L. Baker, Warner and Jenkins[8, 9], Distin, Hallit and Richardson[10], L. Baker and Ward[11] and R. Baker[12] to obtain information on the oxidation of impurities in iron alloy droplets.

On the other hand when molten steel is poured through air, oxygen picked up by the metal from the atmosphere reacts with other elements dissolved in the steel to form products of reoxidation. In continuous casting, the metal is exposed to an air atmosphere as it passes from the ladle to tundish and from the tundish to the mold. The contamination of ingots by reoxidation products is more serious in continuous casting because rapid solidification prevents the inclusions from floating out. For making cleaner steel, it is therefore necessary to prevent oxidation during these stages. Efforts have been made by Little, Van Oosten and McLean[13] to determine

4

the extent of reoxidation during these stages.

Generally the following experimental techniques have been employed to study the gas-metal droplet reactions.

1. Droplets levitated in an inert atmosphere, exposed to an oxidizing gas for a predetermined length of time and then quenched[8-10].

2. Droplets levitated in an inert gas atmosphere, allowed to fall through an oxidizing atmosphere and then quenched[11].

3. Droplets formed by melting the end of a wire, of known composition, in an inert atmosphere, allowed to fall through an oxidizing atmosphere and quenched[12].

In method 1 the relative velocity between the droplet and the gas remains constant with time. In methods 2 and 3 the droplet velocity increases significantly with time.

L. Baker et al[8, 9] used method 1 to study the kinetics of decarburization of levitated Fe-C alloys. They levitated droplets of molten iron-carbon alloys in a stream of oxygen or carbon dioxide bearing gas, and measured decarburization rates. It was shown that at high carbon concentrations the decarburization reaction took place at the droplet surface and the overall reaction rate was controlled by the rate of diffusion in the gas boundary layer next to the droplet. At low carbon concentration they observed a shift in controlling step such that carbon diffusion in the droplet became significant. In an oxygen stream of sphere Reynolds number equal to 24 (calculated at the film temperature) the shift in control occurred at about 1% C. At this point the nucleation of carbon monoxide began within the droplet and intermittent swelling was observed. The decarburization rate decreased from then on. This point corresponds to the beginning

of mixed control: the rate of carbon diffusion and/or interfacial reaction became significant in relation to the rate of gaseous diffusion.

L. Baker and Ward[11] studied the decarburization rates of free falling iron-carbon alloy droplets (method 2). In their experiments single droplets of about 4 mm. diameter were reacted during free fall through 3 ft. of oxygen. The droplets initially contained carbon in the range between 0.8 and 4.5% C. It was observed that a carbon boil and the associated metal particles ejections occurred at all carbon concentrations. The boil intensified as the carbon concentration decreased, and destruction of the droplet by explosion occurred at about 0.5% C. The subsurface nucleation of CO occurred at much higher carbon concentrations for Fe-C droplets falling in oxygen than for levitated droplets. However while carbon diffusion was significant in the case of falling droplet than the levitated droplet, it was shown that carbon removal rates were in reasonable agreement with those predicted for the gaseous diffusion control.

Distin et al.[10] studied the oxidation of Fe-C droplets levitated in the following gases flowing at various speeds: O_2, CO_2, $O_2 + H_2O$, $A + H_2O$. Under the conditions investigated, it was shown that the rate of decarburization were controlled by mass transfer in the gaseous phase. The conditions under which a free oxide phase forms on the surface of the levitated droplets were established and observations were made on the carbon-oxygen boil. It was observed that the rate of vaporization of metal from the droplet during decarburization in oxygen was somewhat greater than levitation in argon. The fume produced during decarburization appeared to become much denser towards the end of an experiment after free

oxide formed on the surface of the droplet.

R. Baker[12] studied the oxidation kinetics of free falling droplets of Fe-C, Fe-Si, Fe-Mn, Fe-C-Si, Fe-C-Mn, Fe-4% C-Si-Mn and Fe-S alloys using the wire melting technique (method 3). It was observed that over 80% of the metalloids were removed from binary or Fe-Si-Mn-C alloys during a free fall of 5 ft. in oxygen, provided the droplet size was less than 3 mm. in diameter, and the initial silicon and/or manganese content was less than 3%. The metalloids removal rate decreased with increased droplet size. A passive film was formed on the droplet containing more than 6% Si, and no metalloids removal occurred. It was shown that carbon removal was very dependent on the droplet size. Provided the conditions were suitable for desiliconization, the presence of up to about 3% Si accelerated carbon removal, especially from the larger droplets.

Most of these works have been concerned mainly with iron alloys, of composition closer to that of Blast furnace iron, and have neglected the oxidation kinetics of relatively pure iron droplets. The only experimental work concerning the oxidation kinetics of pure iron droplets has been carried out by Distin et al. In their experiments, droplets of iron were levitated in an inert gas atmosphere then exposed to an oxidizing gas (25% CO_2, Balance Argon) for the desired time and quenched in water. The temperature of the specimen during the experiment was in the range 1785°C - 1791°C. The results obtained by Distin et al. are shown in Fig. 1. Under these experimental conditions, internal stirring, due to the electromagnetic field, would have a strong effect on the uniformity of composition within the droplet and the stability of the oxide film on the surface. Moreover, the water used as the quenchent was found to
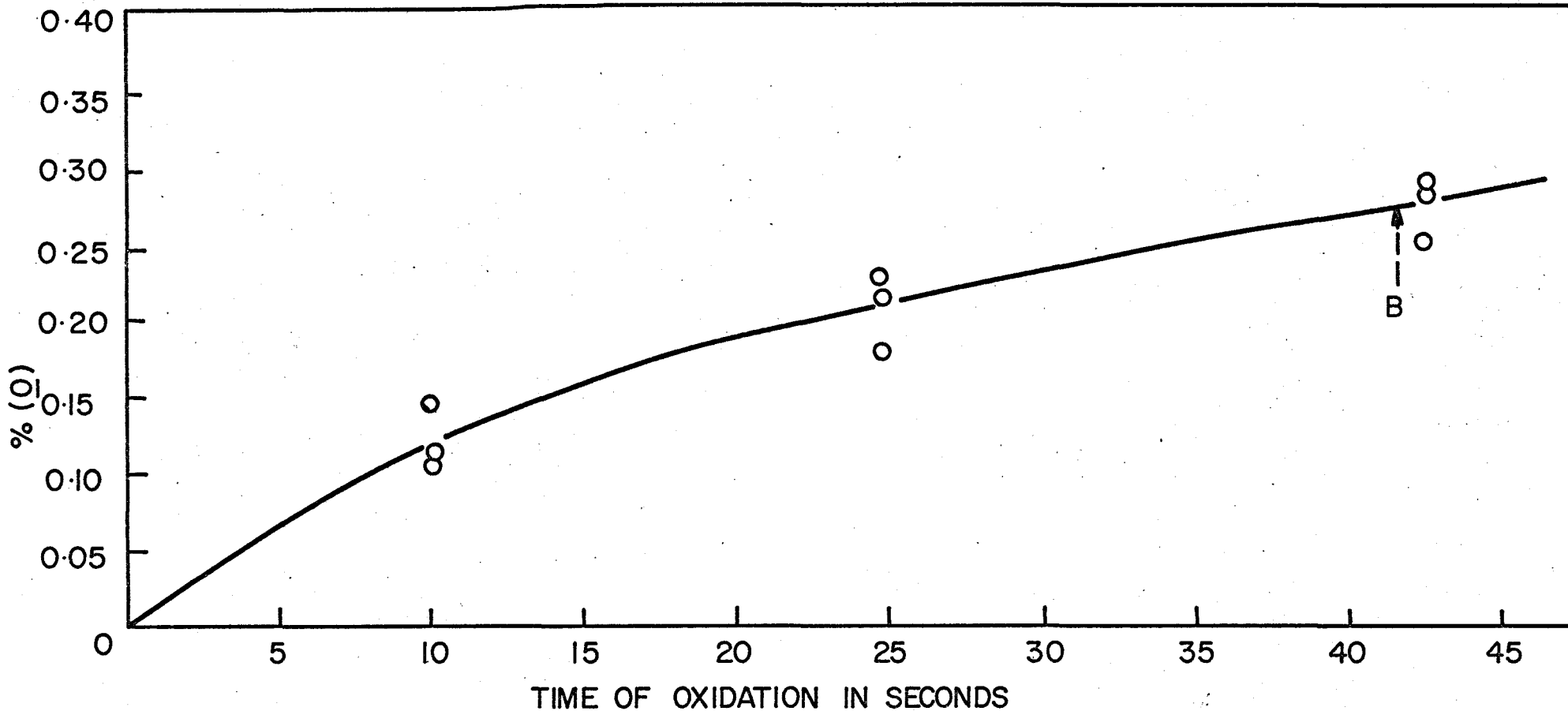
FIG I: COURSE OF OXIDATION OF 1gm. SPECIMEN OF PURE IRON HELD IN A+25%CO_2 FLOWING AT 100cc.min^{-1}. FREE OXIDE APPEARED ON THE SURFACE AT 'B' (REFERENCE 10).

be highly oxidizing with respect to iron at high temperatures.

This study has been designed to investigate the fundamental
nature of oxidation kinetics of free falling iron droplets in an atmosphere
of various oxygen concentrations. The experimental approach will be
discussed in the following chapters.

CHAPTER III

EXPERIMENTAL CONSIDERATIONS

A levitation melting technique was the obvious approach to the present study because of its simplicity and ability to have the metal specimen falling through the oxidizing gas. This technique has been adopted by many authors in kinetic studies of iron alloys reacting with a gaseous phase[8-11]. The design of the apparatus for the present investigation was similar to that used by L. Baker and Ward[11].

3.1 Materials

A description of the materials used is given below.

3.1.1. Armco Iron:

The Armco iron used was in the form of 1/4" diameter rod and was obtained from the Corey Steel Company. The analyses of Armco iron, provided by the supplier, is given below

$$
\begin{array}{lll}
C & - & 0.024 \quad \text{wt. pct.} \\
Mn & - & 0.042 \quad \text{wt. pct.} \\
P & - & 0.007 \quad \text{wt. pct.} \\
S & - & 0.019 \quad \text{wt. pct.} \\
Si & - & 0.000 \quad \text{wt. pct.} \\
0 & - & 0.089 \quad \text{wt. pct.}
\end{array}
$$

3.1.2. Oxidizing Gases:

The reaction gases, of the following composition, were obtained from Matheson Gas Company.

Gas # 1   10% O_2 Balance N_2

Gas # 2   30% O_2 Balance N_2

Gas # 3   20% O_2 Balance Argon

Gas # 4   Air

The gas analysis was checked using a Gas Chromatograph. The maximum error was $\pm$ 5% of the values indicated.

3.2 Levitation Coil:

Various coil designs, each with its own peculiar features, have been tried in the past. A detailed description of the coil designs and their effect on the temperature and stability of the droplet have been discussed in literature[14-16].

In this study a six turn coil of 1/8" i.d thin walled copper tubing was used. The coil was made of two sections (Fig. 2). The lower section of four turns was made by winding two coplaner bottom turns on a conical former with a semi-angle of 30 degrees. The upper section of two turns was wound on the same former but in the reverse direction. This form of the coil was found to give good stability and the desired temperature to the droplet.

The power to the levitation coil was provided by a Toccotron high frequency generator, supplying 10 Kw at 450 Kc/s. A 7.5 : 1 step down transformer was placed between the generator and the coil, thus providing a higher current intensity to the coil. It had the further advantage of suppressing any discharge in the reaction tube.

3.3 Temperature Measurements:

The temperature of the droplet was measured using a precalibrated Milletron - Two Colour Radiation - Pyrometer. The temperatures measured

STABILIZING
PART

30°

15mm

THE FORMER

15 mm

30°

LEVITATING
PART
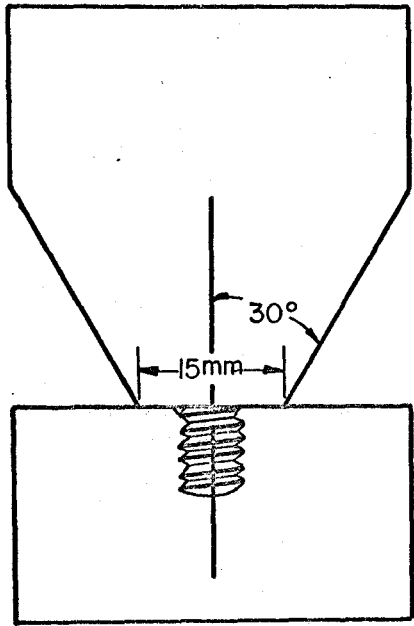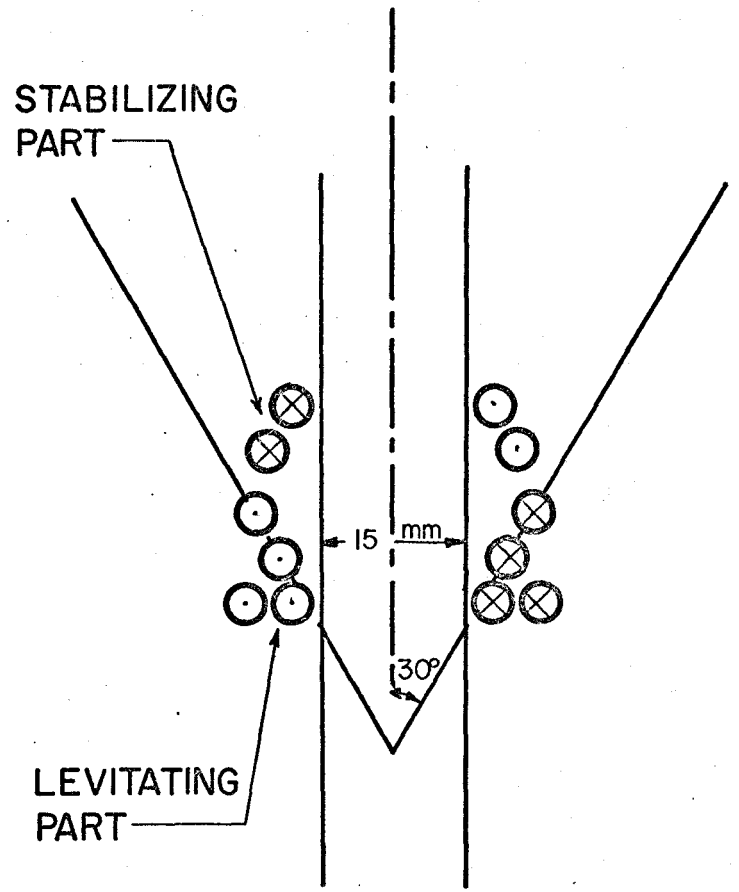
THE COIL

FIG. 2 :

were within $\pm$ 10°C. This instrument measures temperature as a function of the ratio of the intensities at two particular wavelengths. The measurement is thus independent of any variation in emissivity and also of any absorption of rays because of the ratio principle.

The pyrometer was calibrated against a Pt - 5% Rh/Pt - 20% Rh thermocouple dipped into an induction heated Armco iron melt. The calibration apparatus is shown in Fig. 3 and is self explanatory.

The charge of about 100 gms. of Armco iron was placed in a XN 10 Alumina crucible. The melt was heated by an induction coil connected to a high frequency generator (10 Kw, 450 Kc/s). Melting was done in an atmosphere of hydrogen in order to minimize the oxidation. After melt-down the thermocouple was dipped into the melt and the power input to the coil was held constant until the potentiometer gave a steady reading. When this steady state was reached the potentiometer and the pyrometer readings were taken simultaneously. The fact that the potentiometer was grounded and the main crucible had a graphite susceptor around it, made it possible to take the potentiometer reading when the power was on.

Numerous readings were taken while heating and cooling the melt. The calibration curve between the thermocouple temperature and the pyro-meter temperature is shown in Fig. 4.

3.4 Temperature Control:

In a levitated droplet, the heat is produced by I^2R losses of the current induced in it. Hence the temperature of the droplet is largely controlled by the characteristics of the magnetic field and the position of the droplet in the field produced by the coil. The factors which directly

GAS INLET

45°-90° PRISM RADIATION PYROMETER

BRASS FITTINGS

"O" RINGS

ALUMINA THERMOCOUPLE SHEATH

Pt-5% Rh / Pt-20% Rh THERMOCOUPLE

INDUCTION COIL

XN10 CRUCIBLE

GRAPHITE SUSCEPTOR

XN20 CRUCIBLE

ARMCO IRON MELT

ALUMINA POWDER

XN50 CRUCIBLE (SHEATH)

ALUMINA SUPPORT

STEEL TUBE

VYCOR TUBE

BRASS FITTINGS

SWAGELOCK FITTINGS

GAS OUTLET
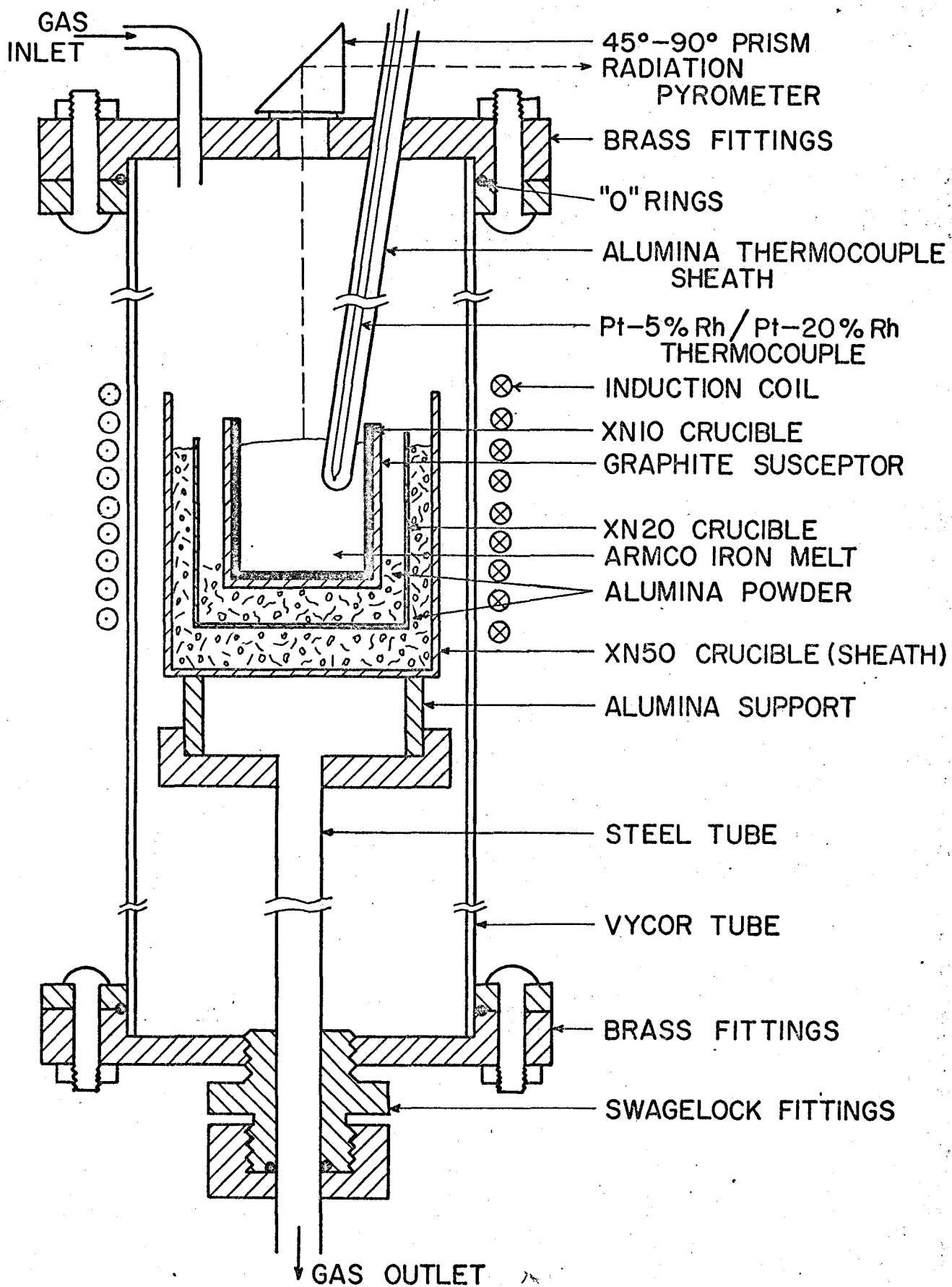
FIG. 3   PYROMETER CALIBRATION APPARATUS.
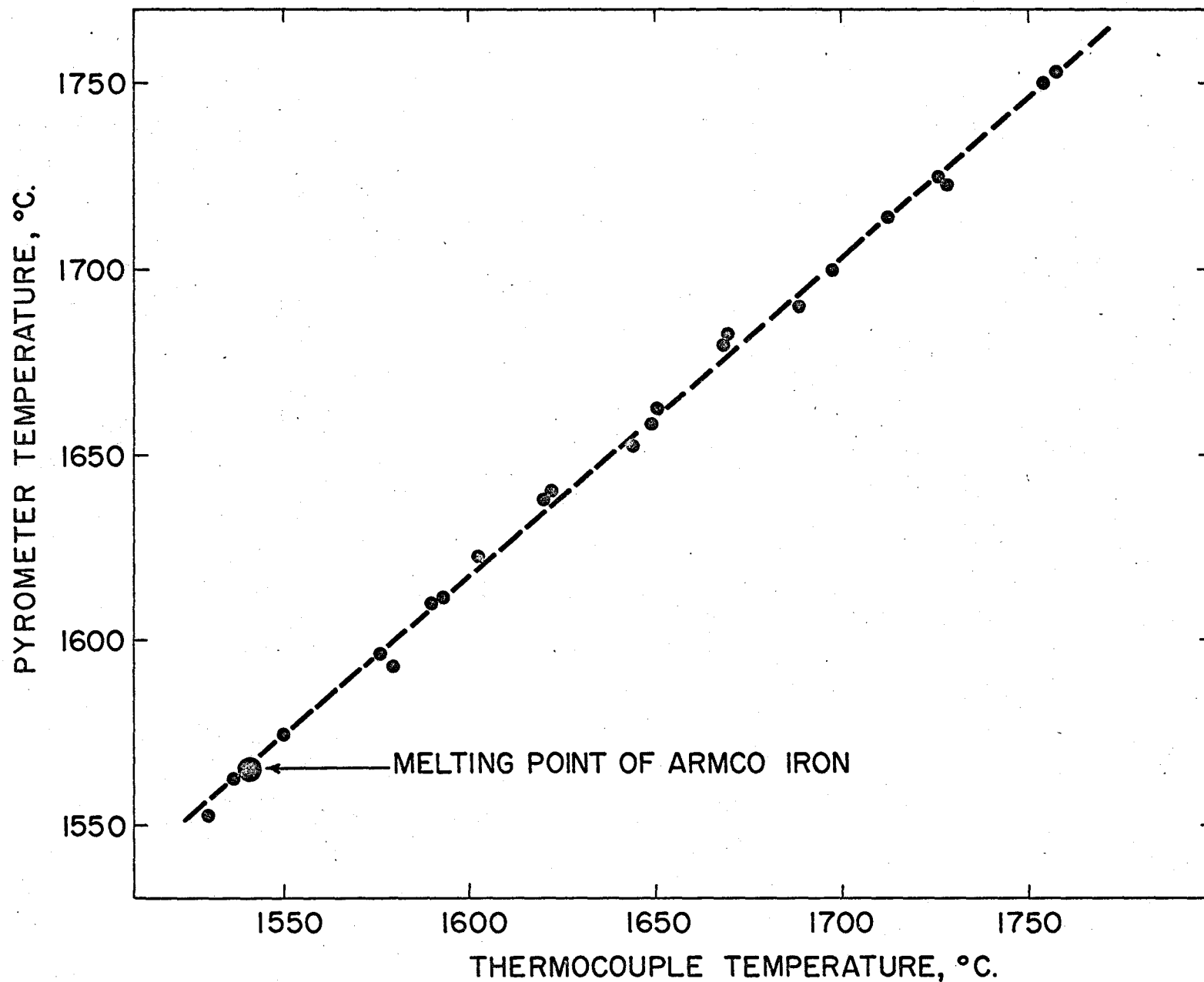
FIG. 4 :   PYROMETER CALIBRATION CURVE .

affect the position of the droplet in the field, and thus the temperature of the droplet, are given below:

1. Power input to the coil

2. Coil design

3. Weight of the sample

4. Electrical and magnetic properties of the specimen.

In addition the heat losses (Convection and Radiation) largely depend upon the gaseous environment (composition and flow rate). By a suitable combination of these factors, the desired temperature can be attained. Jenkins, Harris and Baker[16] studied the effect of these factors on the droplet temperature.

In the present investigation, for a given coil design, the temperature was essentially controlled by adjusting the power input to the coil keeping the other factors constant.

3.5 Quenching Technique:

The selection of a proper quenching medium was a difficult problem. The quenching techniques used in previous studies[8-12] of this kind could not be employed in the present investigation. The quenching medium could not be either reducing or oxidizing under the experimental conditions. Water, as used by R. Baker[12] and Distin et al.[10], was found to be very oxidizing. When the deoxidized Armco iron droplets, weighing about 1 gm., were quenched in water without falling through the reaction chamber (Fig. 5), an oxygen content of more than 650 ppm was found in the quenched specimens. (The experimental procedure will be discussed in the next chapter).

Quenching in a copper mold as used by L. Baker et al.[8] and Little et al.[13] was not feasible because of splashing.

In the first few experiments liquid nitrogen was used as a quenchent, but the results obtained were not reproducible. In order to test the usefulness of liquid nitrogen as a quenchent, a few blank runs were conducted in which hydrogen deoxidized droplets, weighing about 1 gm, were collected in liquid nitrogen placed just beneath the levitation chamber, i.e., the droplets did not pass through the reaction chamber. The oxygen content of such droplets was found to be more than 300 ppm. A similar set of blank runs was made by collecting the droplets in silicone oil placed just beneath the levitation chamber. The oxygen content of the quenched specimens in this case was found to be less than 30 ppm. To check the silicone oil as a reducing agent, specimens of Armco iron of known oxygen content (890 ppm) were levitated in an inert gas atmosphere and quenched in the silicone oil. Droplet temperatures of 1580°C and 1638°C were used. The oxygen content of the quenched specimens was found to be within $\pm$ 50 ppm of the initial specimens. Hence 704 Silicone Oil was selected as the quenching medium in this study.

The silicone oil was obtained from Dow Corning Company, Limited. The quenchent (oil) was Tetra methyl - Tetraphenyl - Trisiloxane having a chemical formula

$$
\begin{array}{ccccccc}
 & & CH_3 & & CH_3 & & C_6H_5 \\
 & & | & & | & & | \\
CH_3 & - & SiO & - & SiO & - & SiO & - & C_6H_5 \\
 & & | & & | & & | \\
 & & CH_3 & & C_6H_5 & & C_6H_5
\end{array}
$$

$$\text{i.e.} \quad (CH_3)_4 \quad (C_6H_5)_4 \quad (SiO)_3$$
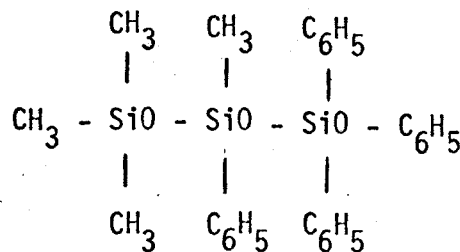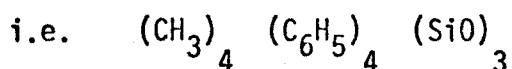
3.6 Oxygen Analyses:

The oxygen analyses were performed on a LECO oxygen analyser. In this method, the sample of metal to be analysed is dropped into a heated graphite crucible where the oxides are reduced in the presence of excess carbon. The resulting CO, which contains all the oxygen in the sample, is then swept by an inert gas, over an oxidizing agent where the CO is converted to CO_2. The resulting CO_2 is then swept into a collection trap. After a preset time the collection trap is heated, the gases are released and carried into a packed column. All three gases pass over a thermal conductivity cell and the change of resistance due to the thermal conductivity of CO_2 is read on a digital voltmeter which gives the wt.pct oxygen in the sample. A schematic diagram of the analyser is given in Appendix A.

Before analysing any sample for oxygen the instrument was calibrated against standard samples furnished by LECO. The reproducibility of the apparatus in the best working condition was about $\pm$ 5 ppm. However the absolute value depends largely upon the reliability of the standards, which were supplied by LECO.

The procedure followed was the one recommended by the manufacturers.

3.7 Carbon, Nitrogen and Silicon Analyses:

3.7.1. Carbon Analyses:

The carbon analyses were done on a LECO gasometric analyser (Orsat analyser). The procedure followed was the one given in the manual which was supplied by the manufacturers.

3.7.2. Nitrogen Analyses:

Nitrogen analyses were carried out according to a report of BISRA on the determination of nitrogen in steel[17]. In this method the substance to be analysed is decomposed with HCl and digested with H_2SO_4 to convert the nitrogen to ammonium sulphate. The ammonia which is liberated by the addition of excess NaOH, is distilled off and absorbed in boric acid solution, the resulting ammonium borate is titrated with standard HCl.

3.7.3. Silicon Analyses:

Silicon analyses were done by the perchloric acid method and the procedure was the one suggested by the ASTM[18].

CHAPTER IV

APPARATUS AND EXPERIMENTAL PROCEDURE

The apparatus was designed to study the rate of oxygen pick up by a droplet of iron falling through an oxidizing atmosphere. In order to interpret the data, experimental conditions such as initial oxygen content of the droplet, relative velocity between the droplet and the oxidizing gas, and the duration of reaction must be known. Droplets of known size and composition were formed and deoxidized in a levitation apparatus. The initial velocity at the moment of entering the oxidation chamber, which was located underneath the levitation chamber, was calculated from the distance of free fall before that time. The total oxidation time was obtained from a knowledge of the initial velocity and the length of the oxidation chamber. The quenching medium was located at the lower end of the oxidation chamber in order to preserve the composition of the droplet at that time. Rates of oxygen pick up were determined by chemical analysis of the quenched specimens.

4.1. Experimental Apparatus

A schematic diagram of the apparatus is shown in Fig. 5. The levitation chamber was made up of three sections. The middle section consisted of a 12 mm. i.d. quartz tube with an inner of 14/23 pyrex joint fixed at its top end and an inner of 24/40 joint fixed at its bottom end. Quartz was preferred to pyrex because it had a high softening point and tolerated a limited contact of molten iron without shattering. A six turn levitation coil was mounted externally to this quartz tube (Fig. 5).

FIG. 5 EXPERIMENTAL APPARATUS

TO RADIATION PYROMETER

GAS OUT

QUARTZ TUBE

LEVITATED DROPLET

LEVITATION COIL

LEVITATION CHAMBER

WATER

He or H_2 IN

POLYTHENE DIAPHRAGM

45/40 JOINT

OXIDIZING GAS OUT

OXIDATION CHAMBER

45/40 JOINT

OXIDIZING GAS IN

SILICONE OIL
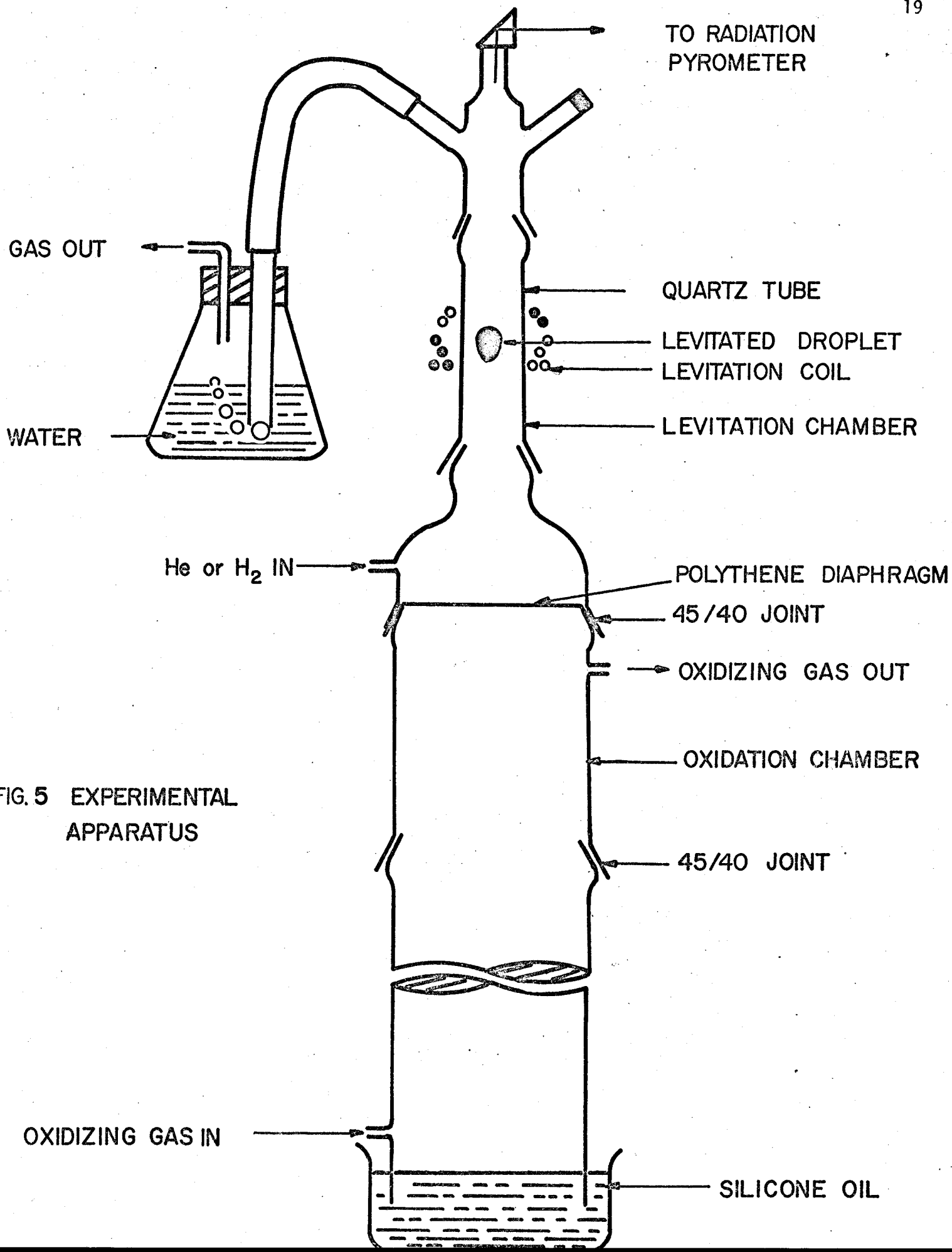
The upper section, with outer of 14/23 joint fixed at its lower end, had two side arms and a thin stem tube. A 45° - 90° prism was placed on top of a glass window fixed at the top end of the stem tube. The lower section had outer of 24/40 joint fixed at the top end and outer of 45/40 joint fixed at its bottom end. The upper and lower sections were made of pyrex glass tubes.

The levitation chamber was separated from the reaction chamber by a separating diaphragm. This diaphragm was placed between the two chambers by using a 45/40 pyrex joint. The outer part of this joint was fixed to the bottom of the levitation chamber and the inner part was fixed to the top of the oxidation chamber. The diaphragm material was polythene which decomposed as the droplet approached and a neat hole was formed as the droplet passed through.

The reaction chamber was made up of 1.8 inches i.d. pyrex tubes about 11 inches long, joined together by using 45/40 pyrex joints. In this way any desired height of the reaction chamber could be achieved. The droplet after reaction for a given time, was quenched in 704 Silicone Oil placed in a beaker just beneath the reaction chamber.

4.2 Experimental Procedure:

4.2.1. Sample Preparation:

After cleaning the superficial oxide layer the rod was cut into samples weighing about 1 gm. The rough edges of the sample were smoothed on a sand grinder. The samples were then washed with acetone and stored in a Desiccator until used.

4.2.2. General Levitation Procedure

The usual procedure for a run was as follows:

With the coil empty, the H.F. power was brought to the maximum and the specimen was raised into the coil on a glass rod and levitated. Helium was continuously flowing through the levitation chamber so as to minimize the oxidation during melting (Fig. 6). As soon as the specimen was molten, the separating diaphragm was placed in position (Fig. 5). The gas flow in the levitation chamber was then switched to hydrogen. Although experience in past indicated that only two to three minutes were necessary to deoxidize the droplet in hydrogen, nevertheless the hydrogen was passed for five minutes to ensure that the droplet was completely deoxidized. Usually the hydrogen deoxidized droplet contained less than 10 ppm oxygen. As the droplet was undergoing deoxidation the required height of the reaction chamber was adjusted by joining glass tubes of suitable lengths with 45/40 joints. The desired oxidizing gas was then passed through the reaction chamber at 550 c.c. per minute.

After deoxidizing the droplet for five minutes in hydrogen, the gas atmosphere in the levitation chamber was switched back to helium and the desired droplet temperature was obtained by adjusting the power input to the coil. The droplet was released by switching off the power and quenched in silicone oil. The reacted specimen was washed with acetone, dried, weighed and analysed for oxygen content by the LECO oxygen analyser.

4.3 Estimation of Reaction Time:

Accurate measurement of the reaction time could not be made directly. It was, therefore, calculated as follows:

TO RADIATION PYROMETER

QUARTZ TUBE

SPECIMEN
LEVITATION COIL

LEVITATION CHAMBER

WATER

He IN

He OUT

GLASS CHARGING ROD
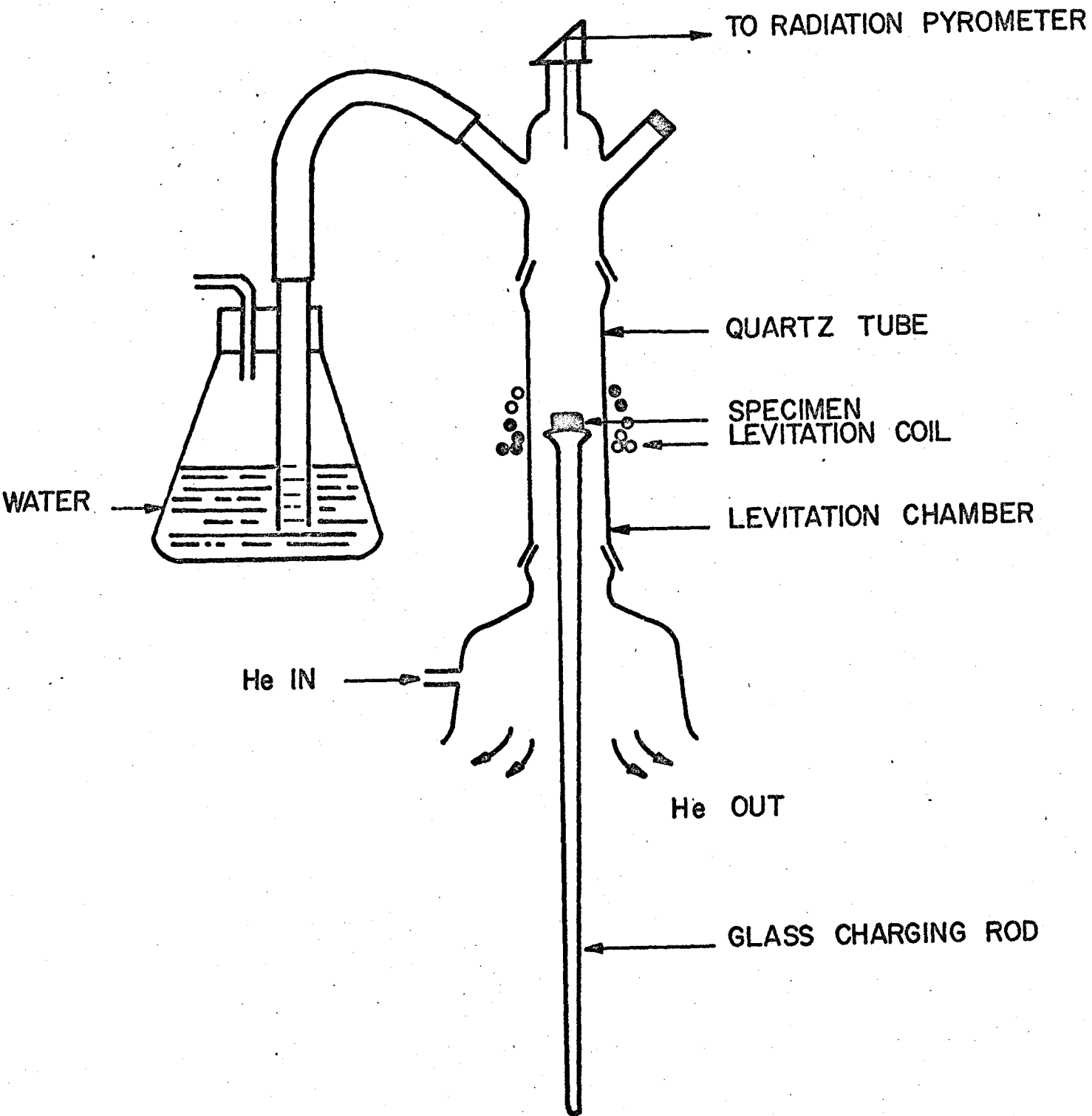
FIGURE 6 .   SPECIMEN CHARGING

A force balance on an accelerating droplet may be expressed as

$$M_d \cdot \frac{dv}{dt} = M_d \cdot g - M_g \cdot g - \text{Drag Force} \qquad \ldots \ldots \ldots \quad (1)$$

Where v -   the velocity of the droplet relative to the gas in cm/sec.

M_d -   the mass of the droplet in gm.

M_g -   the mass of the gas displaced by the droplet in gm.

g -   gravitational constant in cm/sec^2.

t -   the fall time in seconds.

d -   droplet diameter in cm.

ρ_d -   droplet density in gm/cm^3.

$M_d \cdot g$ -   the gravity force

and $M_g \cdot g$ -   the buoyant force

The drag force is equal to

$$\left(\frac{1}{2} \cdot \rho_g \cdot v^2 \cdot \frac{\pi d^2}{4} \right) \cdot C_D$$

Where ρ_g is the gas density in gm/cm^3.

and C_D is the dimensionless drag coefficient.

For Reynolds numbers up to 1000, the drag coefficient C_D may be expressed as[19]

$$C_D = \frac{24}{R_e} + \frac{4}{R_e^{1/3}}$$

Where Reynolds number $R_e = \dfrac{\rho_g \cdot v \cdot d}{\mu_g}$

μ_g = Viscosity of the gas in poise.

Hence equation (1) may be rewritten as

$$\frac{dRe}{dt} = \left(\frac{g \cdot \rho_g \cdot d}{\mu_g}\right) - 3\left(\frac{\mu_g}{d^2 \cdot \rho_d}\right) \cdot (6.Re + Re^{5/3}) \quad \ldots \ldots (2)$$

which gives the velocity or Reynodls number as a function of time for an accelerating droplet.

Also we know that velocity is the rate of change of distance with respect to time i.e.

$$\frac{dH}{dt} = v$$

Where H is the distance travelled or fall height in cm.

Replacing v by Re gives

$$\frac{dH}{dt} = \left(\frac{\mu_g}{\rho_g \cdot d}\right) \cdot Re \qquad \ldots \ldots (3)$$

Equations (2) and (3) were solved simultaneously using the Fourth order Runge-kutta method to give the fall height and Reynolds number as a function of time. Appendix B shows the computer programme written for this purpose.

Note that there exists a continuity in velocity (but not in the Reynolds number) and a discontinuity in gas properties at the separating diaphragm. In equations (2) and (3) the gas properties were calculated at the film temperature. The film temperature being defined as the arithmetic mean of the droplet temperature and the bulk temperature.

4.4 Effect of Parameters:

The effects of the following parameters on the oxidation kinetics were studied.

4.4.1. Initial Temperature of the Droplet:

Initial droplet temperatures of 1580°C, 1638°C, 1698°C and 1755°C were used. The oxidizing gas was air.

4.4.2. Oxygen Concentration of the Oxidizing Gas:

The following gas mixtures were used:

$$10\% \quad O_2 \qquad Balance \ N_2$$
$$30\% \quad O_2 \qquad Balance \ N_2$$

Air

Pure oxygen

In all the cases the oxidation studies were conducted at an initial droplet temperatures of 1580°C, 1638°C and 1755°C.

4.4.3. Size of the Droplet:

This was achieved by using specimens of differenct initial weights. Specimens of Armco iron of average weights 0.87 gm., 1.08 gm., 1.22 gm. and 1.45 gm. were used. The maximum deviation in the weights indicated was within $\pm$ 0.05 gm. The initial droplet temperature, used in all cases, was 1638°C.

4.4.4. Effect of Nitrogen

In order to determine the effect of nitrogen on the oxidation kinetics, nitrogen analyses of various specimens were carried out. The specimens had an initial droplet temperature of 1638°C and 1755°C and were reacted in air for various times.

Experiments, at a droplet temperature of 1638°C, were performed by replacing all the nitrogen in the oxidizing gas with argon. The oxygen analyses of these quenched specimens were performed as discussed before.

4.5 Metallographic Studies

A few quenched specimens, after reaction (oxidation), were mounted and polished by usual metallographic procedure. Examination of these specimens under a microscope (magnification X 500) revealed very small black particles (about one micron in size), well distributed throughout the specimen.

Considerable effort was made to identify these black particles. The techniques generally employed for this purpose are discussed by Ridal et al[20]. The method involving chemical or electrical dissolution was not suitable in the present case because of very low oxygen content in the quenched specimen.

4.6 Electron Probe Micro-Analysis:

Attempts were made to identify these particles by using an electron probe micro-analyser. The specimen preparation for this purpose did not

differ fundamentally from the ordinary polishing methods for metallographic studies, but the last polishing step with alumina paste was not performed.

As the oxides are non-conducting, it was necessary to make the sample surface conducting, otherwise a standing charge would build up on the oxide particles. This would cause instability in the electron beam and prevent accurate analysis. A thin layer of carbon was, therefore, deposited on the polished specimen surface by an evaporation technique.

4.7 Measurement of Reaction Time:

The reaction time (oxidation time) was measured by filming the falling droplet using the HYCAM high speed camera. Films were taken at 1060 frames/sec by focussing the camera at different positions in the oxidation chamber with a ruler in the view.

When the droplet fell from 40.5 cm. fall height (i.e. the distance from the separating diaphragm) to 44.5 cm. fall height in the oxidation chamber, the measured time was 0.0141 sec. The estimated time (section 4.3) under the same experimental conditions was calculated to be 0.0135 sec.

When the droplet fell from 10.62 cm. fall height to 18.62 fall height in the oxidation chamber, the measured time was 0.0406 sec. The estimated time under the same experimental conditions was 0.0385 sec.

It was therefore concluded that the measured times were within $\pm$ 5% of the estimated times.

CHAPTER V

RESULTS

Most of the results are given in a tabular form indicating the oxygen pick up (in wt. pct.) by the droplet as a function of fall height and reaction time under various experimental conditions. The values given in the tables are the mean of as many as ten values obtained by analysing quenched specimens reacted under the same conditions. The values in the parenthesis give the range of oxygen pick up for each fall height.

5.1 Effect of Temperature:

Table I and Fig. 7 show the oxygen pick up by the droplet as a function of fall height, and hence the reaction time, at various temperatures.

The quenched specimens with initial droplet temperatures of 1580°C and 1638°C were of symmetrical spherical shapes with a flat bottom, indicating that they were still liquid on touching the bottom of the beaker containing silicone oil. The specimens with initial temperatures of 1698°C and 1755°C however were flatter and irregular in shape.

As can be seen from Figure 7 the initial oxidation rate at higher temperatures is low. This could be due to the fact that at higher temperatures the evaporation rate is greater. When the droplet was levitated at 1755°C, fumes could be clearly seen and were carried away by the flowing gases. After the run, the quartz tube of the levitation chamber was brownish in colour.

TABLE I

Oxygen Pick Up in Air as a Function of Fall Height

- Effect of Initial Droplet Temperature

Average Weight of the Droplet = 1.08 gms.
(d = 6.653 mm.)

Height of fall in air (inches)	Time of oxidation (seconds)	Oxygen Pick Up in wt. pct.			
		Initial Droplet Temperature			
		1580°C	1638°C	1698°C	1755°C
6.5 inches	0.075.	0.025 (.022 - .027)	0.022 (.020 - .025)	0.0215 (.019 - .023)	0.0160 (.0140 - .0190)
11.00 "	0.115	0.034 (.031 - .036)	0.031 (.029 - .033)	0.027 (.024 - .030)	0.0180 (.0160 - .0190)
22.25 "	0.198	0.044 (.041 - .046)	0.0450 (.042 - .047)	0.0455 (.043 - .048)	0.036 (.035 - .039)
33.25 "	0.268	0.055 (.053 - .057)	0.056 (.053 - .059)	0.059 (.057 - .062)	0.0588 (.057 - .060)
40.00 "	0.300	0.060 (.058 - .064)	0.062 (.060 - .063)	0.065 (.064 - .068)	0.070 (.070 - .072)
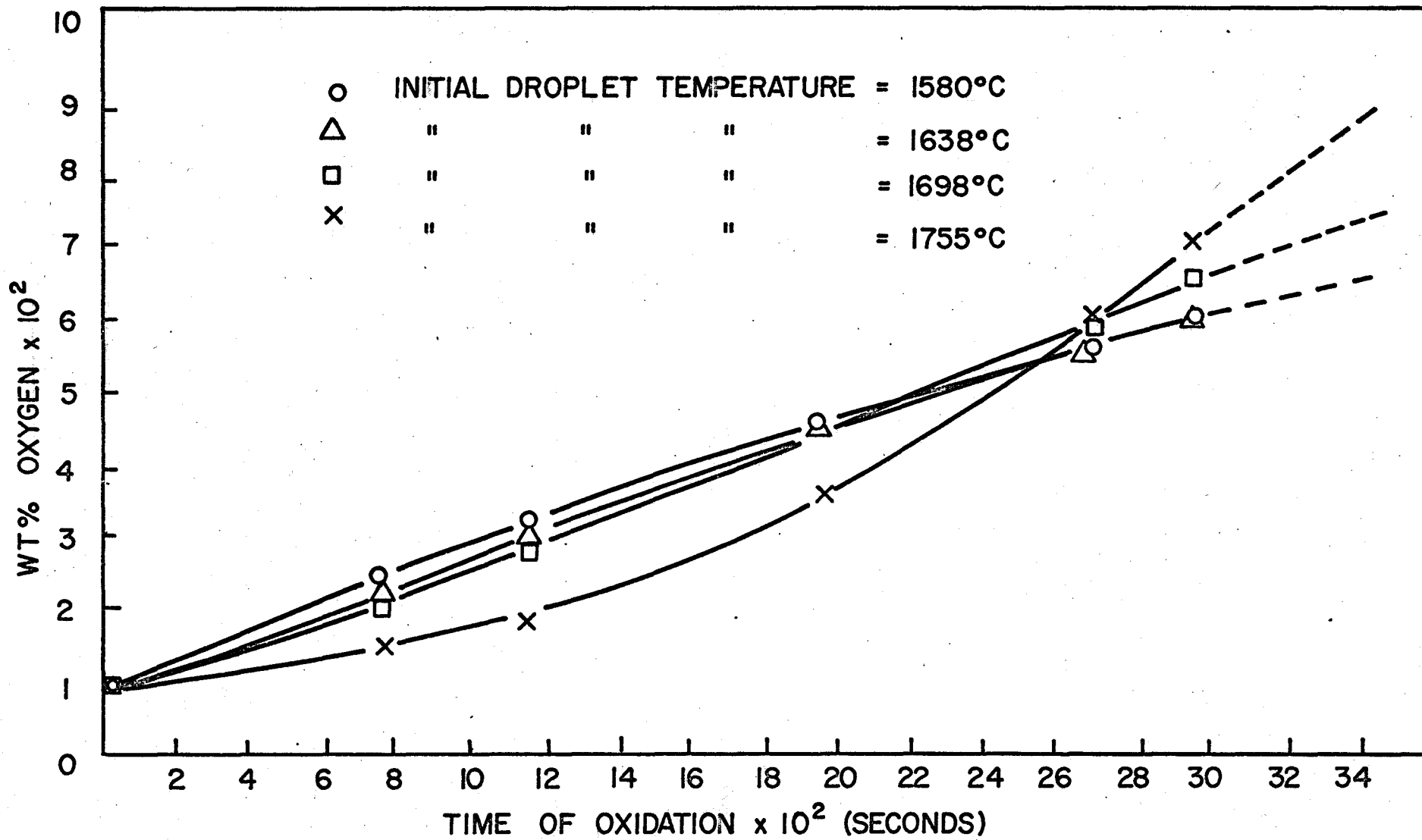
FIG.7. EFFECT OF INITIAL DROPLET TEMPERATURE

5.2 Effect of Nitrogen in the Oxidizing Gas*:

A few experiments were carried out, at initial droplet temperatures of 1638°C and 1755°C, to determine the influence of nitrogen on the oxidation kinetics of droplets falling through air. The initial nitrogen content of the specimen was very small (less than 0.004 wt. pct.). For an initial droplet temperature of 1638°C, the nitrogen pick up by a falling droplet was almost negligible (on an average 0.004 wt. pct. $\underline{N}$ for a fall height of 11" in the oxidation chamber) and did not increase with reaction time. At an initial specimen temperature of 1755°C the nitrogen concentration of the droplet, for a fall height of 11 inches in the oxidation chamber, increased to an average value of 0.015 wt. pct. Again the nitrogen concentration did not increase further with the reaction time.

Further experiments were performed using an oxidizing gas mixture of 20% oxygen, balance Argon. The initial droplet temperature used was 1638°C. Figure 8 shows the results obtained in comparison with air as the oxidizing medium. It may be noted from this figure that when nitrogen was replaced by argon there was no effect on the oxidation rate of the iron droplets.

5.3 Effect of Oxygen Concentration in the Oxidizing Gas:

Tables II and III show the dependence of the oxidation rate on temperature for 10% O_2 and 30% O_2 in the oxidizing gas respectively. The

---

*   This part of the work was done in collaboration with P. Coates, an
    undergraduate student in the Department of Metallurgy and Materials
    Science, McMaster University, Hamilton, Ontario.
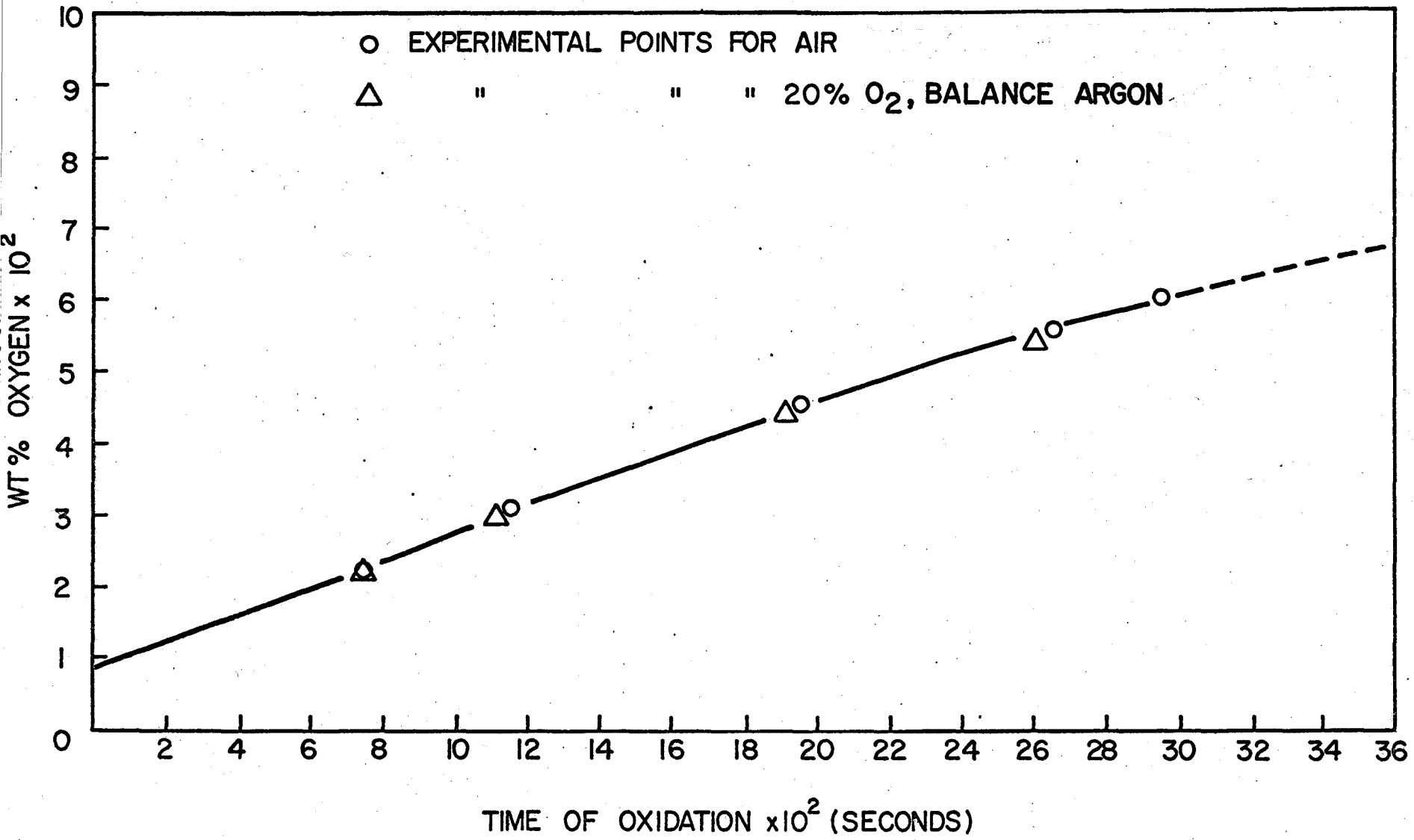
FIG. 8. EFFECT OF NITROGEN

average weight of the specimens in all cases was 1.08 gm.

A few runs were made with 100% oxygen as the oxidizing gas. The oxygen pick up by the droplets with initial temperatures of 1638°C and 1755°C are tabulated in Table IV. At an initial droplet temperature of 1638°C, sparks were observed to come from the droplet after it had fallen for about 25 inches in the oxidation chamber, and finally it exploded at about 30 inches fall height. Explosion of the droplet occurred at about 20 inches fall height when the initial droplet temperature was 1755°C. Since the atmosphere above the quenching oil was pure oxygen, the oil ignited whenever a droplet exploded. All these factors made it difficult to study the oxidation kinetics for larger fall heights, with pure oxygen as the oxidizing gas.

Figures 9, 10 and 11 show the plot of wt. pct. oxygen in the droplet as a function of reaction time for different oxygen concentrations in the oxidizing gases at 1580°C, 1638°C and 1755°C respectively.

5.4 Effect of Droplet Size:

Dependence of the oxygen pick up with respect to the reaction time, for different droplet sizes is given in Table V and plotted in Fig. 12. Droplets of initial average weights 0.88 gm., 1.08 gm., 1.22 gm. and 1.45 gm. were used. The deviation in the weights was within $\pm$ 0.05 gm. An initial temperature of 1638°C was used in all the cases.

5.5 Carbon and Silicon Analyses:

A few quenched specimens with initial droplet temperatures of 1580°C, 1638°C and 1755°C were analysed for carbon. These specimens were obtained by letting the deoxidized Armco iron droplets to fall into

TABLE II

Oxidation Rate as a Function of the Initial Droplet Temperature

Average Weight of the Droplet = 1.08 gm.
(d = 6.653 mm)

Oxidizing Gas: 10% O_2, Balance N_2

Height of fall in oxidation chamber	Time of oxidation (seconds)	Oxygen Pick Up in wt. pct.		
		Initial Droplet Temperature		
		1580°C	1638°C	1755°C
6.5 inches	0.075	0.0210 (.0180 - .0240)	.0205 (.0180 - .0240)	0.0150 (.0120 - .0180)
11.00 "	0.115	0.0265 (.0230 - .0280)	0. 0250 (.020 - .030)	0.0175 (.0160 - .020)
21.25 "	0.194	0.0395 (.0375 - .0415)	0.0420 (.0370 - .0440)	0.0242 (.020 - .0260)
31.75 "	0.257	0.0475 (.0430 - .0510)	0.0520 (.0490 - .0540)	0.0260 (.0245 - .0290)
38.75 "	0.297	0.0520 (.050 - .0540)	0.060 (.0580 - .064)	–

34

TABLE III

Oxidation Rate as a Function of the Initial Droplet Temperature

Average Weight of the Droplet = 1.08 gm.)
(d = 6.653 mm)

Oxidizing gas: 30% O_2, Balance N_2

Height of fall in oxidation chamber	Time of oxidation (seconds)	Oxygen Pick Up in wt. pct.		
		Initial Droplet Temperature		
		1580°C	1638°C	1755°C
6.5 inches	0.075	0.0310 (.0280 - .0330)	0.0295 (.0270 - .0310)	0.0170 (.0150 - .0180)
11.00 "	0.115	0.040 (.0360 - .0430)	0.0354 (.0340 - .0380)	0.0220 (.0195 - .0240)
21.25 "	0.194	0.0535 (.0500 - .0580)	0.0530 (.0510 - .0560)	0.0390 (.0350 - .0430)
31.75 "	0.257	0.0640 (.0600 - .0670)	0.0654 (.0630 - .0680)	0.0660 (.0630 - .0720)
38.75 "	0.297	0.0720 (.0700 - .0740)	0.0720 (.0680 - .0730)	0.0805 (.0770 - .0830)

TABLE IV

Oxidation Rate for 100% Oxygen

Average Weight of the Droplet = 1.08 gm.
(6.653 mm)

Height of fall in oxidation chamber	Time of oxidation (seconds)	Oxygen Pick Up in wt. pct.	
		Initial Droplet Temperature	
		1638°C	1755°C
6.5 inches	0.075	0.0260 (.0230 - .0290)	0.0180 (.0170 - .0220)
11.00 "	0.115	0.0410 (.0390 - .0460)	0.0200 (.0195 - .0205)
21.25 "	0.194	0.150 (.130 - .170)	Exploded
31.75 "	0.257	Exploded	Exploded

FIG. 9 : INITIAL DROPLET TEMPERATURE = 1580°C
EFFECT OF OXYGEN CONCENTRATION OF THE GAS.
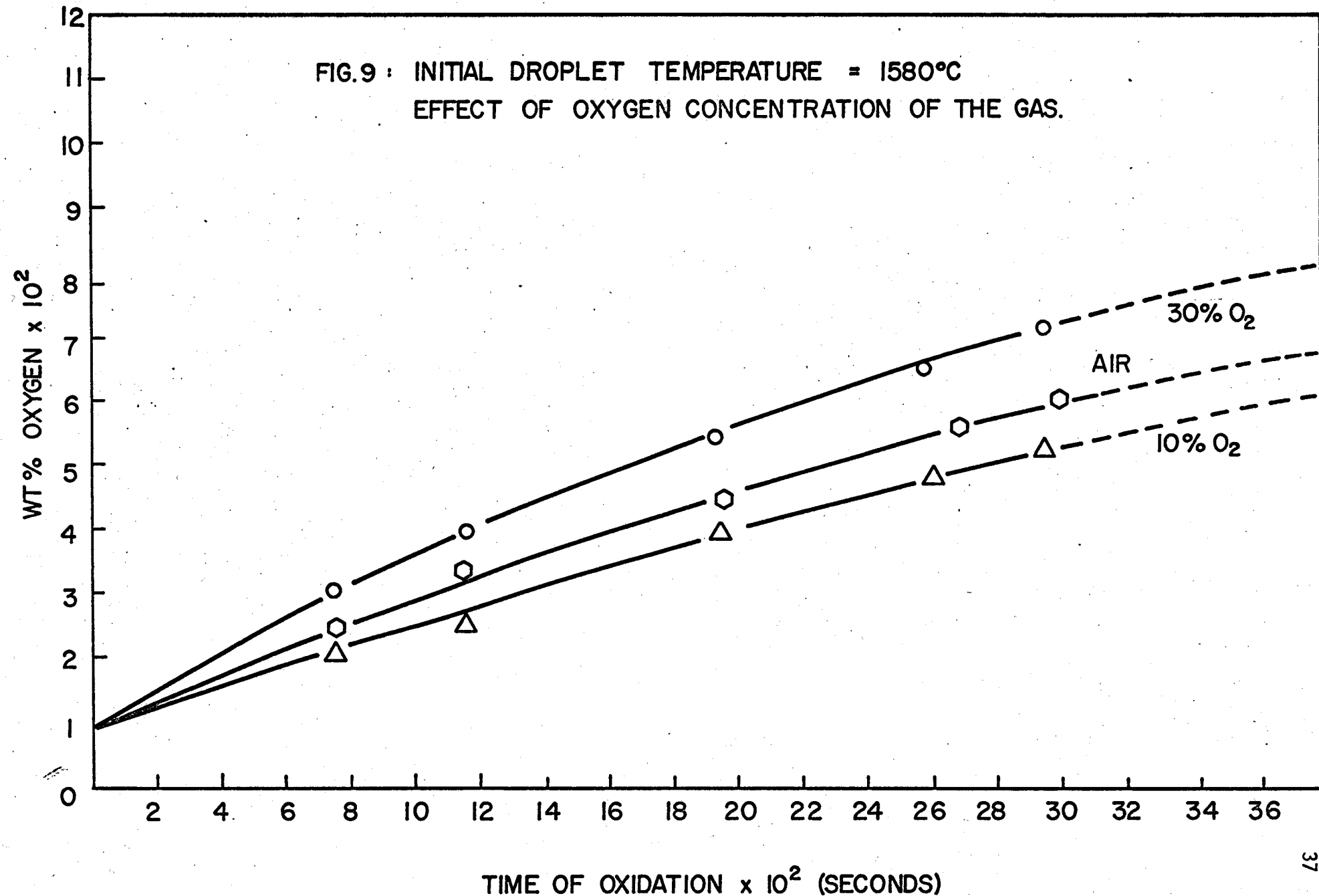
FIG. 10: INITIAL DROPLET TEMPERATURE = 1638°C

EFFECT OF OXYGEN CONCENTRATION OF THE GAS

TIME OF OXIDATION x 10^2 (SECONDS)

FIG.II: INITIAL DROPLET TEMPERATURE = 1755°C
EFFECT OF OXYGEN CONCENTRATION OF THE GAS

30% O_2

AIR

10% O_2

WT% OXYGEN x 10^2

TIME OF OXIDATION x 10^2 (SECONDS)
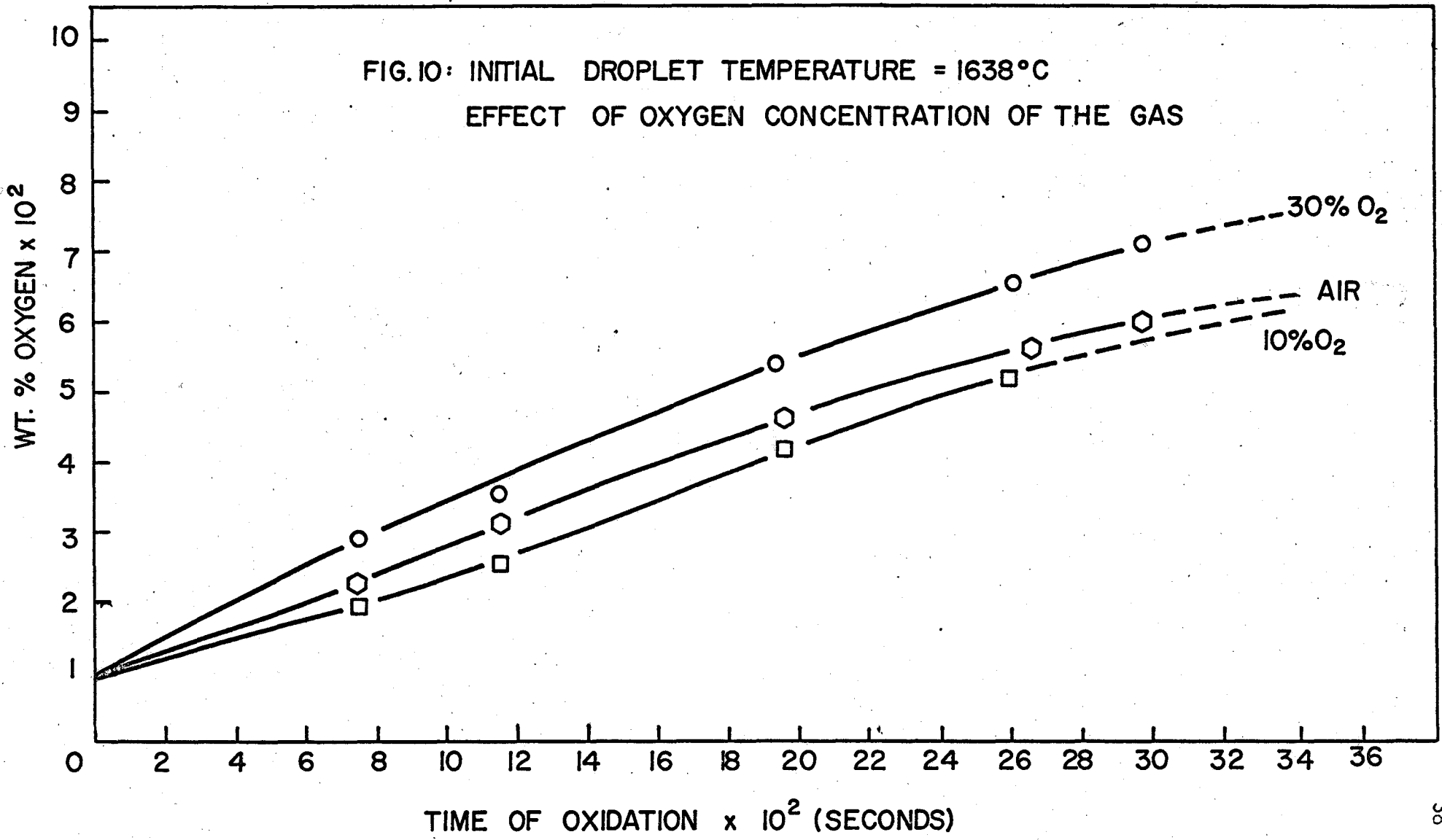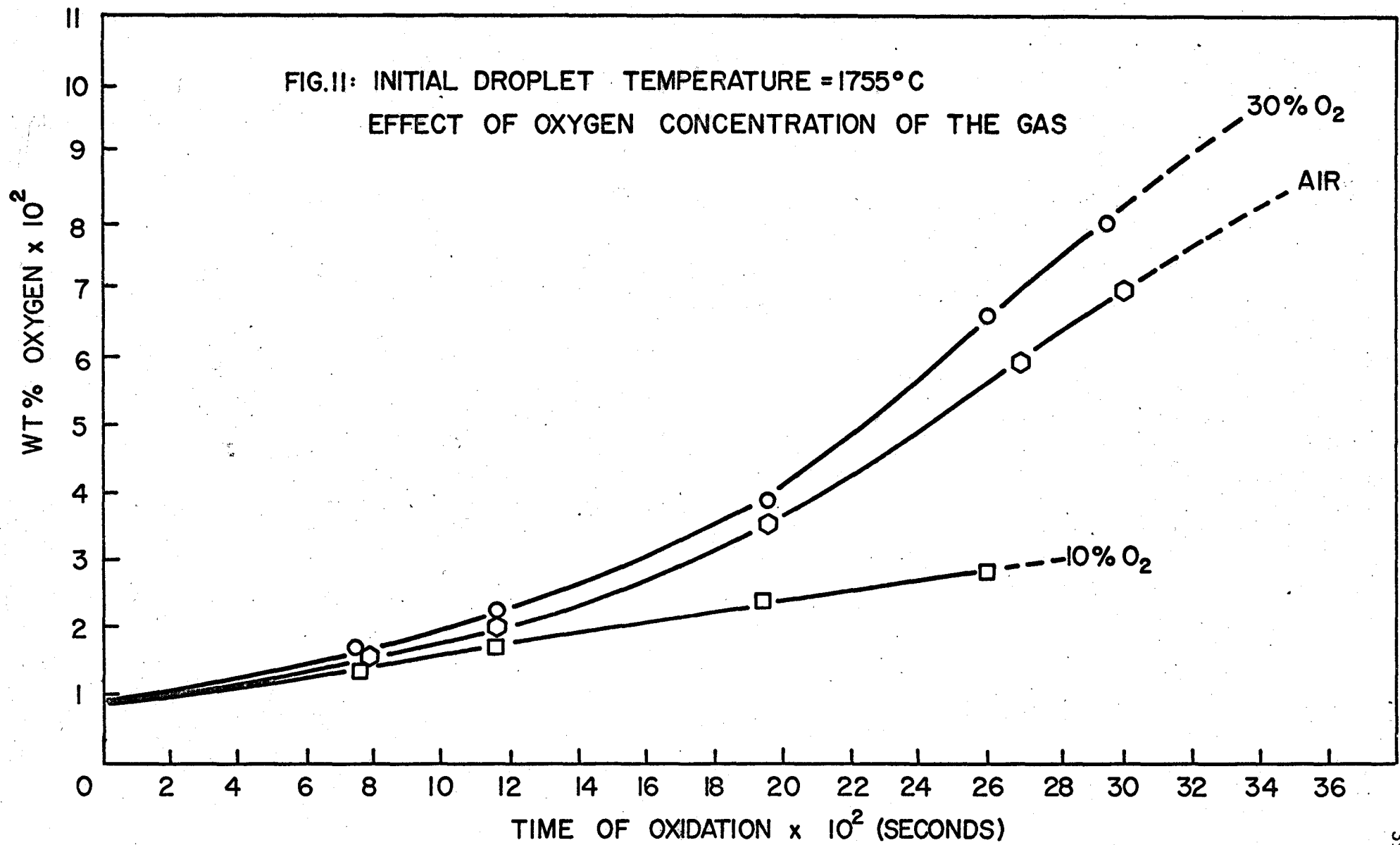
TABLE V

Oxygen Pick Up in Air as a Function of Fall Height

- Effect of Droplet Diameter

Initial Temperature of the Droplet = 1638°C

Oxidizing Gas: Air

Height of fall in oxidizing chamber	Time of oxidation (seconds)	Oxygen Pick Up in wt. pct.			
		Initial Weight of the Droplet			
		0.87 gms. (d = 6.214 mm)	1.08 gms. (d = 6.679 mm)	1.22 gms. (d = 6.955 mm)	1.45 gms. (d = 7.368 mm)
6.5 inches	0.075	0.0229 (.020 - .023)	0.0220 (.020 - .025)	0.0188 (.016 - .020)	0.0170 (.015 -.017)
11.00 "	0.115	0.0360 (.031 - .039)	0.0310 (.029 - .033)	0.0250 (.024 - .027)	0.0310 (.025 - .035)
22.25 "	0.198	0.0474 (.046 - .050)	0.0450 (.042 - .047)	0.0420 (.040 - .045)	0.0376 (.035 - .040)
33.25 "	0.268	0.0600 (.058 - .063)	0.0560 (.053 - .059)	0.0580 (.057 - .060)	0.0480 (.045 - .050)
40.00 "	0.300	0.0700 (.067 - .072)	0.062 (.060 - .063)	0.0610 (.060 - .065)	0.0530 (.051 - .053)

FIG.12. EFFECT OF DROPLET SIZE

(1) — WT. OF THE DROPLET = 0·87 gms. (dia. = 6·214 mms.)
(2) — WT. " " " = 1·08 gms. (dia. = 6·653 mms.)
(3) — WT. " " " = 1·22 gms. (dia. = 6·955 mms.)
(4) — WT. " " " = 1·45 gms. (dia. = 7·368 mms.)

WT % OXYGEN x 10^2

TIME OF OXIDATION x 10^2 (SECONDS)
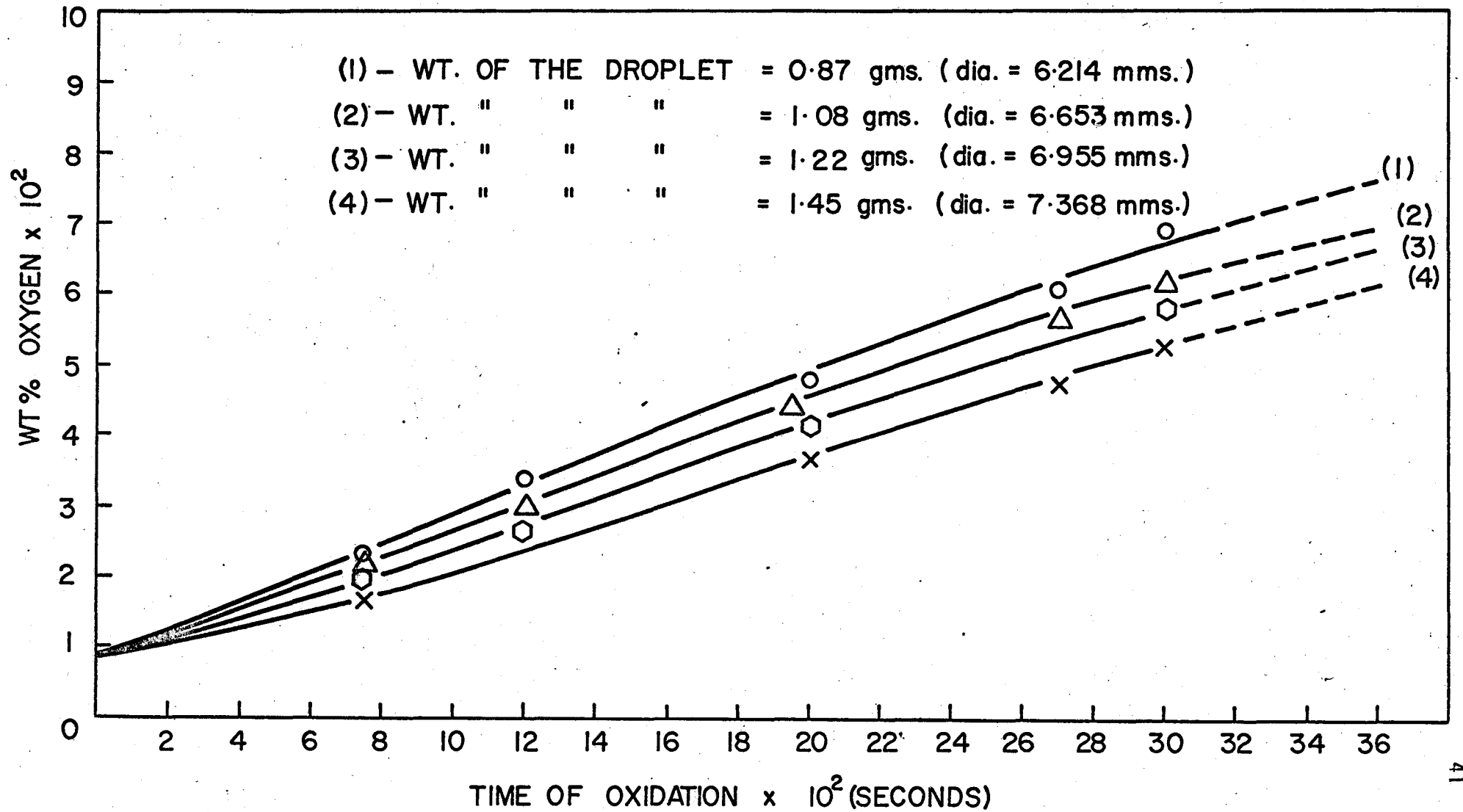
Silicone Oil placed just beneath the levitation chamber. The carbon pick up by the droplet from Silicone Oil at various temperatures is given in Table VI.

TABLE VI

Average Carbon Pick Up at Various Temperatures

Initial Droplet Temperature	Av. wt. pct. Carbon in the Quenched Specimen
1580°C	0.40%
1638°C	0.78%
1755°C	1.10%

Two sets of experiments, with an initial droplet temperature of 1755°C, were conducted by letting the droplets fall through atmospheres of air and of nitrogen respectively. The droplets were collected in Silicone Oil after falling in the reaction chamber for 0.198 seconds. The quenched specimens were analysed for carbon and in both cases the carbon pick up by the droplets, from Silicone Oil, was about 1.1 wt. pct.

Silicon analyses of such quenched specimens indicated that they picked up about 0.25% Si from the oil.

5.6 Metallographic Examination:

Examination of the quenched specimens under a microscope (magnification X 500) revealed very small black particles well distributed throughout

the specimen   (Fig. 13). Similar particles were observed when the
starting material, Armco iron (890 ppm oxygen), was examined   (Fig. 14).

5.7 Electron Probe Micro-Analysis:

When the electron beam was focused on the small black particles,
no oxygen peak was observed. The larger particles, slightly greyish in
colour, showed an oxygen peak indicating that they were oxides. No
oxygen gradient could be observed across the specimen.

Numerous difficulties were encountered while performing micro-
analysis for oxygen. The sensitivity of the instrument was insufficient
to identify the low level of oxygen dealt with in this study. The black
particles thought to be oxide particles were too small for positive
identification.

5.8 Heat Transfer Calculations:

The final temperature of the droplet just before it touches the
quenching medium was calculated. Heat dissipates from the droplet by
convection and radiation. It was found that heat loss by convection
was negligible compared to that by radiation at the temperatures under
consideration.

The temperature of the droplet rises due to the exothermic oxida-
tion reactions. It was assumed that all the oxygen present in the droplet
was in the form of dissolved oxygen and the exothermic reaction that
took place was

$$1/2 \ O_2 \ (g) \ \rightarrow \ \underline{O}(\%) \quad (\Delta H = -28,000 \ cal./gm. \ atom)$$
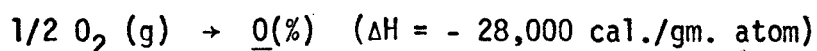
Initial and final droplet temperatures, when the droplet falls in

the levitation chamber for 7 inches and in the oxidation chamber for 33 inches, are indicated in Table VII. The temperatures of the droplet at the separating diaphragm are also shown in Table VII.

TABLE VII

Heat Transfer Calculations Results

Droplet Temperatures		
Initial	Diaphragm	Final
1580°C	1571°C	1560.4°C
1638°C	1628°C	1615.4°C
1698°C	1686.5°C	1671.7°C
1755°C	1742.4°C	1725.2°C

The details of calculation are given in Appendix C.
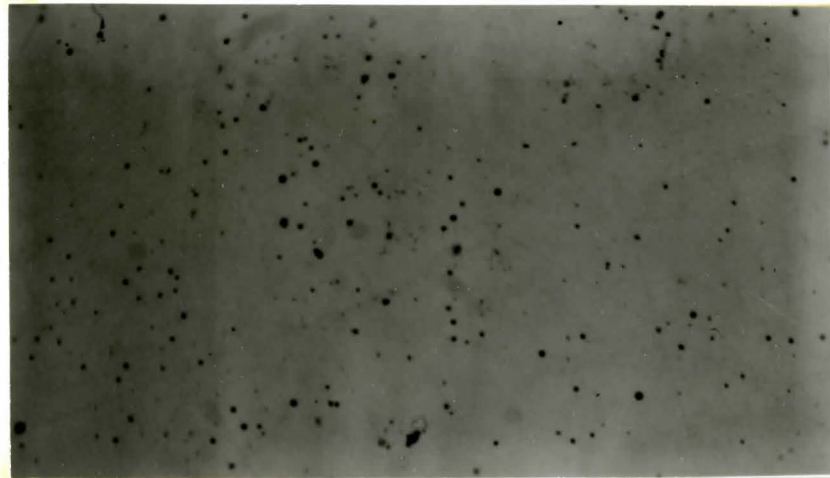
Figure 13 Microphotograph of a quenched specimen. This specimen
was obtained by letting the iron droplet of an initial
temperature of 1755°C to fall in the oxidation chamber
for 0.257 seconds. Not etched.

Magnification X500
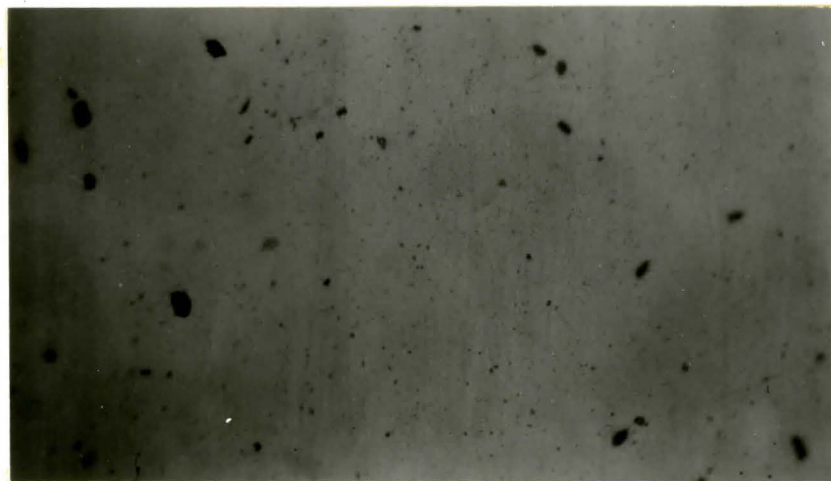
Figure 14 Microphotograph of an Armco iron specimen. Not etched.

Magnification X500

CHAPTER VI

DISCUSSIONS

6.1 Distribution of Oxygen in the Droplet:

The oxygen found in the quenched specimen may be associated with the droplet at high temperature as dissolved oxygen, or partly in the form of oxide, depending upon the extent of oxidation. In the initial stages of oxidation one would expect that all the oxygen is likely to exist in solution and, in the later stages, it is likely to form an oxide layer on the droplet surface. Chemical analysis of the specimen gives an overall composition and provides no information about the concentration profile inside the droplet.

Some attempts were made to determine the oxygen distribution inside the quenched specimen. Results from metallographic studies did not indicate any significant oxide layer on the surface. But on the other hand, tiny black particles could be seen which were well distributed throughout the specimen. These particles were thought to be oxide particles but no positive identification could be made, even by using the electron probe micro-analyser because the size of the particles was very small. Some large particles were identified as oxide particles. No claim on the distribution of oxygen in the specimen could be made on this basis as such a distribution of particles might have occurred during solidification.

6.2 Reaction Rate - Controlling Steps:

In general, the overall reaction takes place in the following steps:

a.) Transfer of reacting species (oxygen) to the gas-metal interface.

b.) Chemical reaction at the interface.

and   c.) Transfer of the reacted species from the interface to the rest of the condensed phase.

In addition, diffusion of the ions in the product phase formed (oxide layer), especially in the later stages of reaction, may be an important step. Generally, one step (which is much slower than the others) or a combination of the aforementioned steps, will control the overall reaction rate.

As discussed before, there was no indication of a significant oxide layer formed on the droplet surface, or of any oxygen concentration gradient in the condensed phase. Hence, at present, it is considered that transport of reacting species in the condensed phase, or of ions in the product phase, is not rate controlling. In the initial stages of oxidation the rate of chemical reaction at the interface would be very high, since the two highly reactive species (iron and oxygen) are meeting at a high temperature. Moreover, in the initial stages of oxidation, the droplet has an open surface for oxygen. Hence the overall reaction rate is not controlled by the chemical reaction at the gas-metal interface.

6.3 Theoretical Model:

For a reaction involving air (or any other mixture of oxygen and nitrogen) there is always a depletion of gaseous oxygen in the neighbourhood of the interface. Therefore the overall oxidation rate may be controlled, to a first approximation, by transfer of oxygen in the gaseous phase.

This is true at all temperatures for the initial period of oxidation. The calculated oxidation rate, based on the above assumption (that the other resistances are negligible) should give a maximum value, which should be equal to or higher than the values observed experimentally. Using a forced convection diffusion model developed by Hamielec, Lu and McLean[19], the rate of change of oxygen concentration of the droplet with respect to the reaction time may be expressed as

$$\frac{d}{dt} \text{ (wt. pct. oxygen)} = \frac{(F \cdot X_{A \text{ bulk}})}{d^2} \cdot (2 + E \cdot R_e^{1/2}) \quad \ldots \quad (4)$$

Where

$$F = \frac{19200 \ P \cdot D_{AB}}{\rho_d \cdot R \cdot T_E}$$

$$E = 0.6 \left(\frac{\mu_g}{D_{AB} \cdot \rho_g} \right)$$

P   -   total pressure of the gas in atm.

R   -   the gas constant in $cm^3 \cdot atm./gm.mole/°K$.

D_{AB} -   Diffusion coefficient of species A in cm^2/sec.

X_A -   Mole fraction of species A in the gas phase at the edge of the concentration boundary layer.

and T_E -   effective temperature in °K

Equations 2, 3 and 4 were solved simultaneously using the Fourth order Runge-kutta method and a CDC 6400 computer to give wt. pct. oxygen in the droplet as a function of reaction time. A computer program for this purpose is given in Appendix B.

A very steep temperature gradient exists around the droplet. Employing the above equations (equations 2, 3 and 4) for a non-isothermal system, introduces difficulties in choosing an effective temperature to calculate the physical properties of the gaseous phase. In addition, for a multicomponent system, it is difficult to estimate an effective diffusion coefficient. Hamielec et al. and other previous workers suggested that the gas properties should be evaluated at the film temperature (defined previously), and the total molar density at the edge of the concentration boundary layer should be evaluated at an effective temperature T_E, where in general $T_E \sim T_f$ for decarburization of falling iron droplets[19].

There is no theoretical justification in the literature for this empirical approach to account for the steep temperature gradient.

Adams[21] suggested that the diffusion coefficient be evaluated at the droplet temperature and molar density at the bulk temperature. However, in his study, a particular velocity profile[22] around the droplet was assumed and no experimental evidence was given to the model proposed.

A complete study of such non-isothermal systems is necessary before any justification for the usage of a film temperature or any other temperature can be made. The development of a mathematical model was not in the scope of this study. Therefore at present the following may be stated.

At the beginning of a kinetic run, the resistance of the chemical reaction and transport process in the condensed phase is negligible, therefore the overall rate should be essentially controlled by mass transfer in the gaseous phase. Such an assumption is more realistic the lower the concentration of oxygen in the bulk gas. By fitting the curve of the mathematical model developed by Hamielec et al. with the experimental data

(for initial stages of oxidation) obtained by oxidizing the droplet with 10% O_2 gas, the undetermined parameter of the model, T_E, was found to be 0.75 T_f. The value of T_E/T_f selected here is lower than that used by Hamielec et al. at a similar droplet temperature. In their system, the exothermic homogeneous reaction

$$CO + \frac{1}{2} O_2 \rightarrow CO_2$$
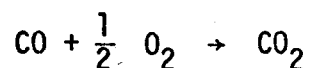
takes place around the droplet. Hence such a difference is expected.

6.4 Comparison of Results:

Figure 15 compares the experimental results with those predicted by the theoretical model for 30% O_2, 20% O_2 and 10% O_2 cases at an initial droplet temperature of 1580°C.

No comparison is shown at other temperatures because the evaporation rate of iron becomes important at higher temperatures. Without the evaporation correction, the model is certainly inadequate for higher droplet temperatures.

As can be seen from Figure 15, the predicted curve lies above the experimental curve for both 30% O_2 and 20% O_2, the difference between the two being greater for 30% O_2 than 20% O_2. This indicates that the resistances other than transfer of oxygen in the gaseous phase become more important for the case of higher oxygen concentration in the oxidizing gas. As expected, in the initial stages of oxidation, the agreement between the predicted and experimental curves (10% O_2) is very good, but as the reaction proceeds, the two curves deviate. This may be explained by the following arguments.
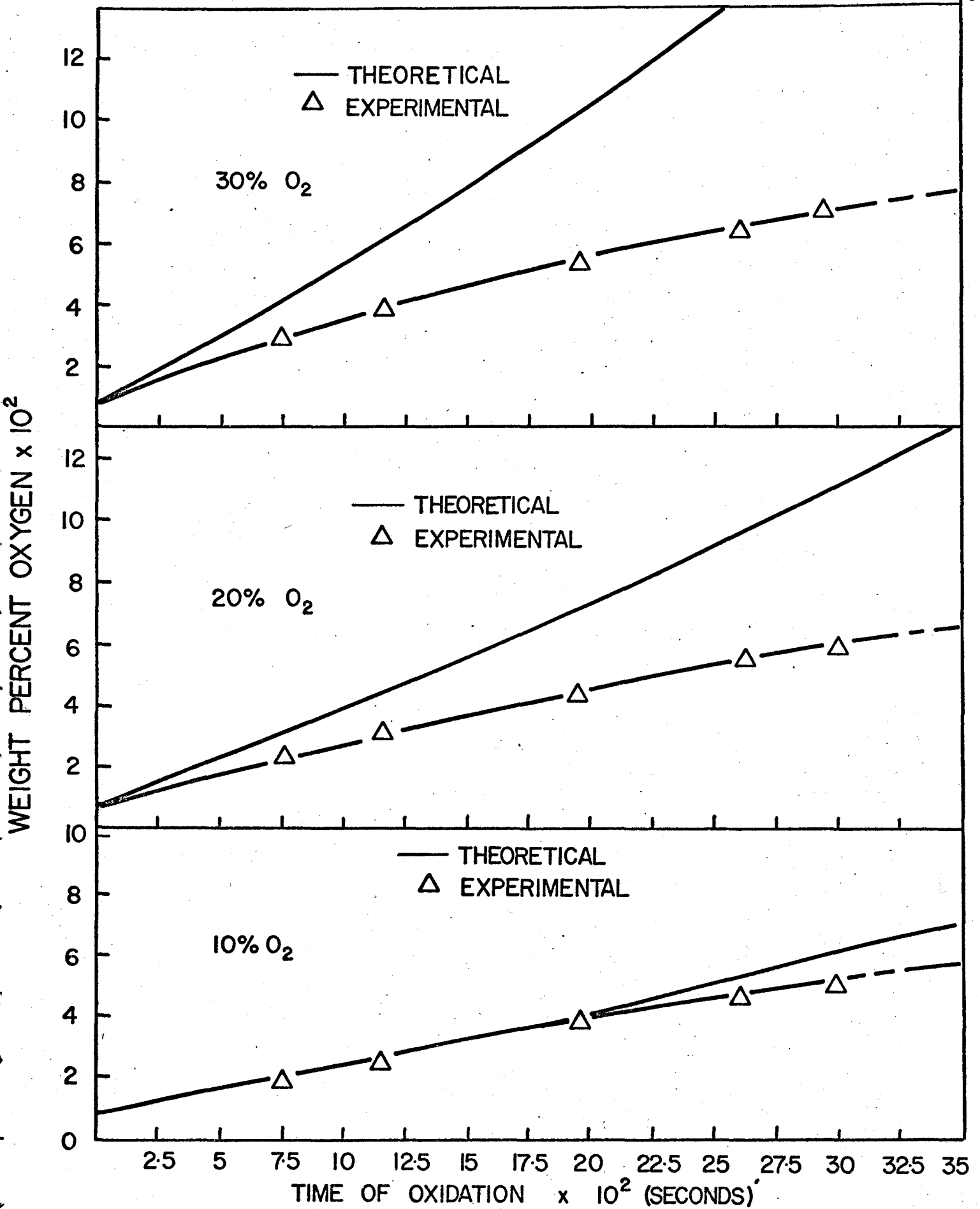
FIG. 15   THEORETICAL AND EXPERIMENTAL CURVES FOR
30%, 20%, AND 10% O_2 IN THE OXIDIZING GAS

When the droplet accelerates, the turbulence in the gaseous phase surrounding the droplet increases and hence the transfer of reacting species on the gaseous side increases. Therefore, in the later stages of oxidation the resistance in the gaseous phase may not dominate any longer and the other resistances may become significant. Also, as the oxidation proceeds the concentration of oxygen at the droplet surface may become greater than the bulk. This could happen due to two factors. Firstly, insufficient time was available for oxygen to diffuse into the bulk while the droplet was falling, and secondly, the oxygen is surface active. Hence in the later stages of oxidation the resistance in the condensed phase or chemical reaction at the interface may become important.

6.5 Effects of Temperature:

Figure 7 shows the effect of temperature on the oxidation kinetics using air as the oxidizing gas. It may be observed that the initial oxidation rate is slower at higher temperatures, but as the droplet was oxidized for a sufficiently long period, the final oxygen content was greater for higher initial droplet temperatures. Similar effects were observed for the cases when the oxygen concentration was 10% O_2 and 30% O_2.

This phenomenon may be attributed to the fact that the evaporation of iron from the open surface of the droplet is faster for higher initial droplet temperatures $(3.5 \times 10^{-3} g/cm^2$-sec. at 1725°C[29]). Initially, at 1725°C, the outward flux of iron vapor is high and iron vapor is oxidized by intercepting the inward oxygen flux which may otherwise reach the droplet. The oxygen flux reaching the droplet, as indicated by analyses of quenched specimens, is lower than the value predicted by the simple model. However, as the droplet falls, it picks up more oxygen, even though at a lower rate

and its temperature drops. Smith and Ward[23] found that the vapour
pressure of iron decreases with the increase in oxygen content of the
iron. As a result the evaporation rate decreases and therefore the oxygen
content of the droplet increases sharply. For the gaseous mixture of
10% oxygen (Fig. 11) there was not much oxygen pick up by the droplet since
both the oxygen concentration in the gaseous phase and the oxygen flux
were low. The evaporation rate was sufficiently high to consume most of
the oxygen flux on its way toward the droplet.

6.6 Nitrogen Results

As could be noted from the results of nitrogen analyses, the
nitrogen pick up by the droplet was considerably greater at 1755°C
(0.015 wt. pct.) than at 1638°C (0.004 wt. pct.). This may be explained
by considering that at 1755°C the evaporation rate is high and the oxygen
flux reaching the droplet, in the beginning of oxidation, is small. The
droplet is open and reactive with respect to nitrogen. The same is not
true at 1638°C when the evaporation rate is slower and the droplet picks
up oxygen more rapidly. The surface of the droplet is thus no longer free
and open for nitrogen. This agrees with the results of Naeser and Scholtz[24]
who determined that dissolved oxygen had a considerable effect on the dis-
solution rate of nitrogen in liquid iron. The effect of dissolved oxygen
on the mass transfer coefficient of nitrogen has been determined by
Kozakevitch and Urbain[25] who found that in the presence of 0.020% oxygen
the rate of nitrogen dissolution is one twentieth than that for pure iron.

6.7 Evaporation Correction:

At 1725°C the oxygen consumed by the vapour has been calculated

(0.126% $\underline{0}$/sec.) on the assumption that all the iron vapour is oxidized to FeO. Quenched specimens were analysed for nitrogen after falling through various heights of air from an initial droplet temperature of 1755°C. These results clearly indicated that the evaporation of iron is of significance solely for the first 11 inches (reaction time up to 0.115 sec.) of the oxidation chamber. For the case where reaction time was less than or equal to 0.115 sec., the oxygen consumed by iron vapour was added to the final oxygen analysis of the quenched sample. When the reaction time exceeded 0.115 sec., the correction added on the basis that the iron vapour-oxygen reaction occurred for the initial 11 inches only. The results are shown in Fig. 16. It may be noted that after applying the evaporation correction, the oxidation rate curve for 1755°C becomes higher than that for 1580°C, as would be anticipated from the theoretical considerations.

6.8 Effect of Droplet Size:

From Figure 12 it may be observed that the oxygen concentration in the droplet increases faster for smaller droplets because of a larger surface area to volume ratio.
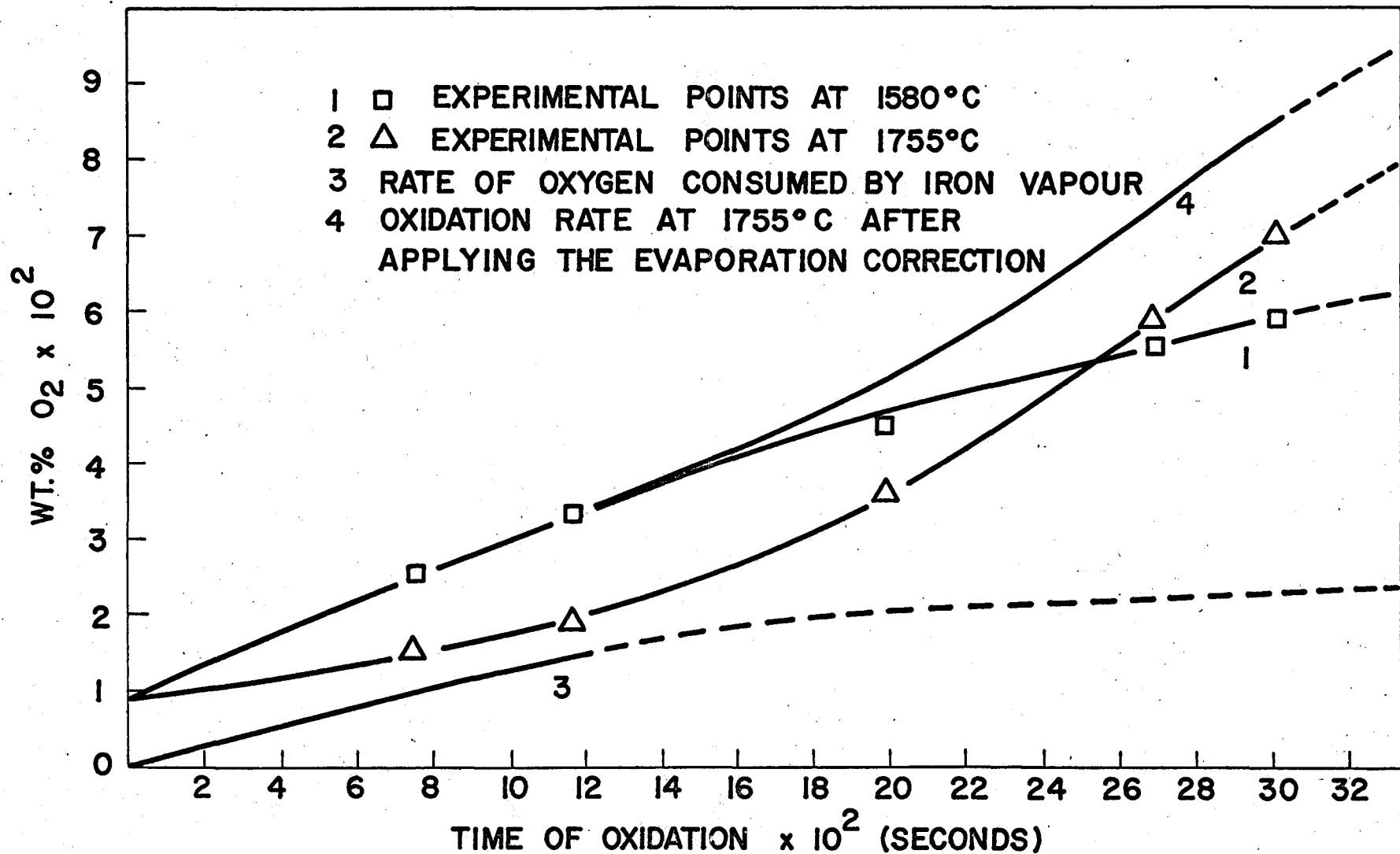
FIG. 16   EVAPORATION CORRECTION

CHAPTER VII

SUMMARY

The oxidation kinetics of free falling iron droplets have been studied over a temperature range of 1580°C to 1755°C, using the levitation technique. As a result of the investigation the following conclusions are presented.

a.) It was found that evaporation of iron is very important and strongly affects the initial oxidation rate of the droplets. The initial oxygen pick up by the droplet, at high initial temperatures, was found to be small as a consequence of significant iron vaporisation.

b.) The overall reaction rate, particularly in the initial period, was found to be controlled by the transfer of oxygen in the gaseous phase, for gas phase composition of 10% by volume of oxygen or less.

c.) The oxidation rate increased as the size of the droplet decreased. This effect was due to the changing surface: volume ratio.

d.) Free falling droplets in pure oxygen exploded. The generation of heat within the droplet was sufficiently strong to produce explosive temperature rises.

56

CHAPTER VIII

SUGGESTIONS FOR FUTURE WORK

Future investigation should include the following.

1. The future work should be extended to iron alloys. In addition to studying iron alloys of composition near to blast furnace iron, emphasis should be given in studying the Fe-Si, Fe-Al, Fe-Mn and Fe-Si-Mn systems. Such work would be helpful towards understanding and perhaps controlling the reoxidation during teeming and casting operations.

The effect of evaporation should be considered when studying the oxidation kinetics of iron alloys at high temperature.

2. Studies with a similar goal should be performed using a different experimental technique, thus eliminating the effect of internal stirring in the levitated droplet due to electromagnetic field e.g. wire melting technique.

3. There is a need to develop a more accurate theoretical model for such non-isothermal systems, when the overall reaction rate is controlled by the transfer of reacting species in the gaseous phase. For a gas-metal system where a very steep temperature gradient exists in the gaseous phase, the fundamental equations for Momentum, Mass and Heat transfer should be solved at each point around the droplet.

589-630 BODY
589-304 NUT
589-305 SLEEVE

589-625
REACTION
TUBE

589-621
UPPER SEAL

589-606 SAMPLE
LOADING DEVICE

507-801 CATALYST
CONNECTOR TUBE

3/16 ID RUBBER TUBING

507-420 CATALYST-
DELIVERY TUBE

589-304 NUT
589-305 SLEEVE

534-352
CRUCIBLE

507-400 FURNACE

507-800
FURNACE

501-92 CARBON BLACK

501-170
CU OXIDE

501-142 ZR SPONGE

GLASS COTTON

GLASS
COTTON

537-236 THIMBLE

589-697 BODY
589-698 NUT
589-699 SLEEVE

534-212 SEAL

534-327 SEAL

DISCONNECT

589-304 NUT
589-305 SLEEVE

589-428
DESICCANT
TUBE ASSY.

537-500
INDUCTION
FURNACE

HELIUM

501-290
NUT

501-286
REGULATOR ASSY.
WITH CU TUBING

516-100
PURIFYING
TRAIN

537-225
PED. TRAY
HOLD. DEVICE

589-600 ANALYZER

501-290 NUT

HELIUM

501-286
REGULATOR ASSY.
WITH CU TUBING

589-303 BODY
589-304 NUT
589-305 SLEEVE

734-300 LECO OXYGEN ANALYZER

APPENDIX - B

C......HAMIELEC ET. AL. FORCED CONVECTION DIFFUSION MODEL ....

```
C         DEFINATIONS

C         TB- BULK GAS TEMPERATURE                    DEG. K
C         TD- DROPLET TEMPERATURE                     DEG. K
C         TF- FILM TEMPERATURE =(TB+TD)/2             DEG. K
C         TE- EFFECTIVE TEMPERATURE                   DEG. K
C         W- WEIGHT OF THE DROPLET                    GM.
C         D- DROPLET DIAMETER                         CM.
C         G- GRAVITATIONAL CONSTANT =980.             CM./SEC.SQ.
C         R- GAS CONSTANT =82.05        CU.CM.ATM./GM.MOLE/DEG.K
C         P- TOTAL GAS PRESSURE                       ATM.
C         RE- REYNOLDS NUMBER
C         DAB- DIFFUSION COEFFICIENT OF SPECIES A    CM.SQ./SEC.
C         XA- MOLE FRACTION OF SPECIES A
C         H- HEIGHT OF FALL IN OXIDATION CHAMBER      CM.
C         T- REACTION TIME                            SEC.
C         AVISC- VISCOCITY OF OXDIZING GAS           POISE
C         HVISC- VISCOCITY OF HELIUM                 POISE
C         GDENS- DENSITY OF THE OXIDIZING GAS       GM./CM.SQ.
C         DDENS- DENSITY OF THE DROPLET             GM./CM.SQ.
C         OX- OXYGEN CONTENT OF THE DROPLET          WT.PCT.
C         HRE- REYNOLDS NUMBER AT THE END OF LEVITATION CHAMBER
C         HH- STEP LENGTH

C.......................OXIDATION KINETICS.....................

C. . . . . . . . . EFFECT OF INITIAL DROPLET TEMPERATURE

          DIMENSION X(5),Y(5),Z(5)
          DO 2 KK=1,4
          READ(5,156)TD,DDENS,HRE
          XA=0.20
          TB=296.
          W=1.08
          TF=(TD+TB)/2.
          TE=0.75*TF
          G=980.
          R=82.05
          P=1.

C ASSUMING THAT AIR BEHAVES AS PERFECT GAS AT HIGH TEMP.

          GDENS=P*28.8/(R*TF)
```

```
C          CALCULATING VISCOCITY OF AIR
C                                    .........CHAPMAN-ENSKOG FORMULA

           ASIG=3.617
           AFUN=0.82
           AVISC=2.6693*(SQRT(28.8*TF))/(100000.*AFUN*ASIG**2)

           DAB=.206*(TF/298.)**1.823
           D=(6.*W/(3.143*DDENS))**.33334

C          DEFINING

           A=G*GDENS*D/AVISC
           B=3.*AVISC/(D**2*DDENS)
           C=(AVISC/(GDENS*D))
           F=19200.*DAB*P/(R*TE*DDENS)
           E=0.6*(AVISC/(DAB*GDENS))**.33334

C          CALCULATING VISCOCITY OF HELIUM
C                                    .........CHAPMAN-ENSKOG FORMULA
           HSIG=2.576
           HFUN=0.584
           HVISC=2.6693*(SQRT(4.00*TF))/(100000.*HFUN*HSIG**2)

C          SOLUTION OF THE DIFFERENTIAL EQUATIONS
C              ..........FOURTH ORDER RUNGE-KUTTA METHOD

C          EQUATIONS TO BE SOLVED ARE...................

C          DRE/DT= A-B*(6.*RE+RE**(5./3.)) ..................(1)
C          DH/DT= C*RE   ....................................(2)
C          D(OX)/DT= (F+XA/D*D)*(2.+E*RE**0.5) .............(3)

C          INITIAL CONDITIONS AT THE BEGNING OF OXIDATION CHAMBER

           HH=0.005
           T=0.
           OX=0.009
           H=0.

C          THE SEPERATING DIAPHRAGM....HENCE EQUIVALENT REYNOLDS
C          NUMBER IN THE OXIDATION CHAMBER IS

           RE=HRE*7.2*HVISC/AVISC

     3     X(1)=HH*(A-B*(6.*RE+RE**(5./3.)))
           Y(1)=HH*C*RE
           Z(1)=HH*(F*XA/D**2)*(2.+E*RE**.5)
           B1=B*(6.*RE+RE**(5./3.))
C          B1 IS THE TERM DUE TO DRAG FORCE
           DO 1 I=2,4
           J=I-1
```

```
       IF(I.EQ.4) GO TO 60
       SRE=RE+X(J)/2.
       GO TO 61
60     SRE=RE+X(J)
61     X(I)=HH*(A-B*(6.*SRE+SRE**(5./3.)))
       Y(I)=HH*C*SRE
1      Z(I)=HH*(F*XA/D**2)*(2.+E*SRE**.5)
       XX=(X(1)+2.*X(2)+2.*X(3)+X(4))/6.
       YY=(Y(1)+2.*Y(2)+2.*Y(3)+Y(4))/6.
       ZZ=(Z(1)+2.*Z(2)+2.*Z(3)+Z(4))/6.
       WRITE(6,10) H,T,RE,OX,A,B1
       OX=OX+ZZ
       H=H+YY
       RE=RE+XX
       T=T+HH
       IF(T.LT.0.40) GO TO 3
        WRITE(6,66) AVISC,HVISC
       WRITE(6,67) DAB
10     FORMAT(3X,F8.3,5(3X,F16.8))
67     FORMAT(1H0,F16.8)
66     FORMAT(1H0,25X,F16.8,13X,F16.8)
156    FORMAT(F6.1,2F6.2)
2      CONTINUE
       STOP
       END
         6400 END RECORD
1853.0  7.00 12.35
1911.0  6.92 11.98
1971.0  6.85 11.65
2028.0  6.78 11.29
         6400 END FILE
```

Heat Transfer Calculations[26,27]

As an approximation, the temperature of the droplet at the moment it entered the oxidation chamber, and at the moment it left the oxidation chamber, was calculated by applying a heat balance at these points. A sample calculation is given below:

1. In Levitation Chamber:

Initial droplet temperature = 1853°K

Weight of the droplet = 1.08 gm.

Diameter of the droplet d = 6.653 mm.

Surface area of the droplet = 1.39 cm^2.

Distance travelled by the droplet in the levitation chamber = 17.8 cm.

a.) Heat Loss Due to Convection:

The convective heat transfer coefficient is given according to the Ranz-Marshall correlation i.e. $Nu = 2.0 + 0.60. Re^{1/2} . Pr^{1/3}$

Where   Nu   -   Nusselt number = $\frac{h.d}{k}$

         Pr   -   Prandtl number = $\frac{C_p . \mu_g}{k}$

         C_p -   Heat capacity in Cal./gm.mole-°K.

         h   -   Convective heat transfer coefficient in Cal.Sec.$^{-1}$.cm^{-2}.°K^{-1}

and   k   -   thermal conductivity of the gas in Cal.sec.$^{-1}$cm.$^{-1}$°K^{-1}

The gas properties were calculated at the film temperature.

Droplet fell in the levitation chamber for 17.8 cm., therefore its Reynolds number, Re, at the end of the levitation chamber = 12.35 (calculated according to Appendix B.)   Prandtl number in helium = 0.90

$$\therefore \quad Nu = 2.0 + 0.6 \, Re^{1/2} \cdot Pr^{1/3} \quad = 4.03$$

Hence $\dfrac{h.d}{k} = 4.03$

$$\therefore \quad h = 3.75 \times 10^{-3} \; cal.sec.^{-1} \; ^{\circ}K.^{-1} \; cm.^{-2}$$

Heat loss by convection = $h \times A \times (1853 - T_H)$ cal./sec.

$$= 5.2125 \times (1853 - T_H) \; cal./sec.$$

Where T_H - the temperature of the droplet in °K at the separating

diaphragm (i.e. at the end of the levitation chamber)

and   A - the surface area of the droplet in $cm.^2$

b.) Heat Loss Due to Radiation

Using the Stefan-Boltzmann correlation, the heat loss due to radiation is given by $\varepsilon.\sigma.T^4$ cal/sec.-$cm.^2$

Where σ = Stefan-Boltzmann constant = $1.355 \times 10^{-12} \; cal.sec.^{-1} cm.^{-2} \; ^{\circ}K^{-4}$

and ε = Emissivity of the droplet = 0.4 for molten iron.

As an approximation, T was assumed to be constant and equal to the initial droplet temperature.

$$\therefore \quad \text{Heat loss by radiation} = 6.38 \; cal./sec.-cm.^2$$

c.) Total Heat Loss by the Droplet:

The total heat loss from the droplet, is the difference of initial and final heat content of the droplet and is given by $\rho_d . \dfrac{\pi d^3}{6} . C_p . \Delta T$.

$$= 0.192 \times (1853 - T_H)$$

and it must be equal to the heat loss due to convection and radiation.

Therefore, applying a heat balance yields: $0.192 \times (1853 - T_H)$

$$= 5.2125 \times 10^{-3} \times 0.19 \times (1853 - T_H) + 6.38 \times 1.39 \times 0.19$$

For the above equation, the solution is $T_H = 1844°K$.

II. In Oxidation Chamber:

Calculation of the heat loss due to convection and due to radiation, in air, were carried out by a procedure similar to that used for calculating heat loss in helium. For the initial droplet temperature of 1844°K at the moment entering oxidation chamber the heat loss due to convection and due to radiation was calculated to be 2.938 cals. when the droplet fell in the oxidation chamber for 33 inches.

Simultaneously with the heat loss due to convection and radiation there is heat gain within the droplet due to exothermic reactions. Assuming that all the oxygen present in the droplet was in the form of oxygen dissolved in the iron according to the reaction;

$$\frac{1}{2} O_2 \text{ (g)} = \underline{O}(\%)$$
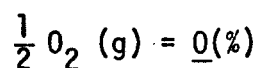
the amount of heat evolved = 28,000 cal/gm. atom.

For an initial droplet temperature of 1853°K, the average oxygen pick up by the droplet was found to be 0.055 wt. pct. for a height of fall of 33 inches and time of fall of 0.27 seconds in the oxidation chamber.

∴ Total heat evolved during this time

$$= 28{,}000 \times \frac{0.055}{1.08} \times 10^{-2} \times \frac{1}{16}$$

= 0.891 cal.

Therefore the net heat loss from the droplet

= 2.938 - 0.891 = 2.047 cal.

Hence the final temperature of the droplet, at the moment leaving the oxidation chamber = 1833.4°K.

Similar calculations were performed using different initial droplet temperatures and the results obtained are shown in Table VII. In all the cases it was found that the heat loss due to convection was negligible compared to that due to radiation.

The above temperatures, calculated by applying the heat balance at two points, are the first approximation to the exact temperatures. A more accurate analysis would involve the calculation of droplet temperature at each point on its path as the droplet falls in the levitation and oxidation chambers. By using such an approach the decrease in temperature would be less than that calculated by applying a simple heat balance principle at two points. This is due to the fact that the heat loss by radiation decreases as the droplet falls in the levitation chamber because of reduction in droplet temperature. Therefore the calculations shown here give the maximum possible decrease in temperature of the droplet. A more accurate analysis was not within the scope of this study.

REFERENCES

1. J. M. Gaines and D. C. Hilty, J. Met., 10, 452, (1958).

2. M. W. Thring, Iron and Steel, 42, 35 (1969).

3. A. Berthet, J. Rouanet and P. Vayssire, J.I.S.I., 207, 790 (1969).

4. J. Pears, Steel and Coal, 185, 506 (1962).

5. J. Pears and J. Pearson, A.I.M.E., O.H. Comm. Proc., 45, 450 (1962).

6. Spray Steelmaking, Iron and Steel, 40, 374, (1967).

7. Spray Steelmaking Technique, British Breakthrough, Steel International October, 159, (1966).

8. L. A. Baker, N. A. Warner and A. E. Jenkins, Trans. A.I.M.E. 230 1228 (1964).

9. L. A. Baker, N. A. Warner and A. E. Jenkins, Trans. A.I.M.E., 239 857 (1967).

10. P. A. Distin, G. D. Hallit and F. D. Richerdson, J.I.S.I., 206, 821 (1968).

11. L. A. Baker and R. G. Ward, J.I.S.I. 205, 714 (1967).

12. R. Baker, J.I.S.I., 205, 637 (1967).

13. J. Little, M. Van Oosten and A. McLean, Can. Met. Quart., 8, 235 (1969).

14. W. A. Piefer, J. Met., 17, 487 (1965).

15. A. J. Rostron, Sci. Journal, 3, 68 (1967).

16. A. E. Jenkins, B. Harris and L. Baker, A.I.M.E. Met. Soc. Conf., 22, 23 (1964).

17. The Determination of Nitrogen in Steel, Special Report No. 62, BISRA Report, Pub. J.I.S.I., London, 36 (1958).

18. ASTM Methods of Chemical Analysis of Metals, Pub. ASTM, 121 (1960).

19. A. E. Hamielec, W-K. Lu and A. McLean, Can. Met. Quart., 7, 27 (1968).

20. A. Ridal, T. K. Jones and R. Cummins, J.I.S.I., 203, 995 (1965).

21. R. Adams, M.Eng. Thesis, McMaster University, (1968).

22. A. E. Hamielec and A. I. Johnson, Can. J. Chem. Eng. $\underline{40}$, 41 (1962).

23. P. N. Smith, M.Eng. Thesis, McMaster University (1965).

24. G. Naeser and W. Scholtz, Stahl Eisen, $\underline{79}$, 137 (1959).

25. P. Kozakevitch and G. Urbain, Memoires Scientifiques de la revue de Metallurgie, $\underline{60}$, 143 (1963).

26. F. Kreith, Principles of Heat Transfer, Pub. International Textbook Company (1966).

27. R. B. Bird, W. E. Stewart and E. N. Lightfoot, Transport Phenomena, Pub. John Wiley and Sons Limited (1966).